

DSIA JOURNAL

A Quarterly Publication of the Defense Systems Information Analysis Center

Volume 1 • Number 2 • Fall 2014

A PROMISING FUTURE FOR US NAVY
**VERTICAL
LAUNCHING
SYSTEMS**

(PAGE 32)

- 05 CARBON NANOTUBES**
Small Structures with Big Promise
- 11 SYNTHETIC APERTURE SONAR**
Improved Technology for Improved Mine Hunting
- 14 Guiding Preventive Maintenance with
WEIBULL ANALYSIS**
- 20 HIGH-POWER MICROWAVE**
Directed Energy Weapons: An M&S Toolbox
- 25 Blast Data Visualization with
PYTHON, PART 1**



Distribution Statement A: Approved for public release; distribution unlimited.

DSIAC JOURNAL

VOLUME 1 | NUMBER 2 | FALL 2014

Editor-in-Chief: Eric Fiore

Contributing Editor: Eric Edwards

Art Director: Melissa Gestido

Cover Photo Credit:

The guided missile cruiser BUNKER HILL (CG-52) test fires an RIM-66C SM-2 missile from the stern Mark 41 Vertical Launching System (VLS) during sea trials (U.S. Navy Photo).

The *DSIAC Journal* is a quarterly publication of the Defense Systems Information Analysis Center (DSIAC). DSIAC is a Department of Defense (DoD) Information Analysis Center (IAC) with policy oversight provided by the Assistant Secretary of Defense for Research and Engineering, ASD (R&E). DSIAC is operated by a team led by the SURVICE Engineering Company and includes Quanterion Solutions Incorporated, Georgia Tech Research Institute, Texas Research Institute Austin, and The Johns Hopkins University.

Copyright © 2014 by the SURVICE Engineering Company. This journal was developed by the SURVICE Engineering Company, under DSIAC contract FA8075-14-D-0001. The Government has unlimited free use of and access to this publication and its contents, in both print and electronic versions. Subject to the rights of the Government, this document (print and electronic versions) and the contents contained within it are protected by U.S. copyright law and may not be copied, automated, resold, or redistributed to multiple users without the written permission of DSIAC. If automation of the technical content for other than personal use, or for multiple simultaneous user access to the journal, is desired, please contact DSIAC at 410.360.4600 for written approval.

Distribution Statement A: Approved for public release; distribution is unlimited.



CONTENTS

- 5** Carbon Nanotubes: Small Structures with Big Promise ▶
AM *Advanced Materials*

- 11** Synthetic Aperture Sonar: Improved Technology for Improved Mine Hunting ▶
MS *Military Sensing*

- 14** Guiding Preventive Maintenance with Weibull Analysis ▶
RQ *RMQSI*

- 20** High-Power Microwave Directed Energy Weapons: A Model and Simulation Toolbox ▶
DE *Directed Energy*

- 25** Blast Data Visualization with Python, Part 1 ▶
SW *Survivability & Vulnerability*

- 32** A Promising Future for US Navy Vertical Launching Systems ▶
WS *Weapon Systems*

CONTACT DSIAC

Thomas L. Moore, PMP
DSIAC Director

Eric M. Fiore, CSEP
DSIAC Deputy Director

DSIAC HEADQUARTERS
4695 Millennium Drive
Belcamp, MD 21017-1505
Office: 443.360.4600
Fax: 410.272.6763
Email: contact@dsiac.org ▶

WPAFB SATELLITE OFFICE
96 TG/OL-AC/DSIAC
2700 D Street, Building 1661
Wright-Patterson AFB, OH 45433-7403
Office: 937.255.3828
DSN: 785.3828
Fax: 937.255.9673

NEW YORK OFFICE
100 Seymour Road, Suite C101
Utica, NY 13502-1311
Office: 315-351-4200

DSIAC CONTRACTING OFFICER REPRESENTATIVES

Brad E. Forch (COR)
U.S. Army Research Laboratory
RDRL-WM
Aberdeen Proving Ground, MD 21005
Office: 410.306.0929

DSIAC PROGRAM MANAGEMENT ANALYST (PMA)

Philippe A. "Phil" Guillaume
IAC Program Management Office (DTIC-I)
8725 John J. Kingman Road, Suite 0944
Fort Belvoir, VA 22060-6218
Office: 703.767.9180
Email: philippe.a.guillaume.ctr@mail.mil ▶

Peggy M. Wagner (ACOR)
96 TG/OL-AC
2700 D Street, Building 1661
Wright-Patterson AFB, OH 45433-7403
Office: 937.255.6302
DSN: 785.6302

MESSAGE FROM THE EDITOR

In an age of increasingly tighter DoD budgets and heightened acquisition

scrutiny, leveraging successes has become more important than ever. One shining example is the U.S. Navy's Aegis Weapon System. This weapon system, which includes the Mk 41 Vertical Launching System (VLS), has racked up a remarkable track record over the past several decades and appears to be poised for an even greater role in fleet protection and ballistic missile defense. In this fall edition of the *DSIAC Journal*, our feature Weapons Systems article presents a historical synopsis of the Navy's VLS and provides a glimpse of emerging research and development (R&D) trends and the expanded roles this exceptional system will fulfill in the future.

Composed of tiny tubular cylinders of carbon atoms, carbon nanotubes (CNTs) are generating a lot of interest in commercial and military sectors with their extraordinary mechanical, electrical, thermal, optical, and chemical properties. Paul Wagner's Advanced Materials article on CNTs discusses current R&D trends and several state-of-the-art applications where these unique structures are demonstrating great promise.

Likewise, the Military Sensing article by Brett Israel and Jennifer Weaver Tate discusses synthetic aperture sonar (SAS) R&D trends being applied to support the Navy's mission of keeping the U.S. fleet safe from submerged mines, which remain an ever-increasing and serious threat. The improved SAS technology also shows great promise to help search for submerged structures, including sunken ships or aircraft, such as the Malaysian commercial airliner that suddenly disappeared last March.

In our Reliability and Maintainability article, Richard Wisniewski discusses the ability of Weibull analysis to guide many preventive maintenance decisions. This analytical approach is commonly used to make predictions about the life of a system for a given population by fitting a statistical distribution to life data from a representative sample. The parameterized distribution of data can be used to estimate important life characteristics of the system, such as reliability or probability of failure at a specific time, the mean life, and the failure rate. This article demonstrates how the application of

this technique can provide a means for assessing the impact and consequence of a failure.

Also, John Tatum's Directed Energy article provides an overview of a few modeling tools currently in use or in development that can help analyze a system's vulnerability and the lethality of current and emerging high-power microwave (HPM) directed energy weapons (DEWs). There is a growing belief that DEW systems are most likely to change the way future battles are planned and fought. Thus, the importance of DEW modeling tools continues to grow as many of these systems edge closer to reality.

Finally, for those readers who might have a hard time grasping the invisible, Will Woodham's Survivability and Vulnerability article is the first of a two-part series on visualizing blast data with the Python programming language. This article includes a few simple examples of code to help transform test data into color graphics. In next quarter's issue, he'll discuss how to generate 3-D animations. So stay tuned. ■

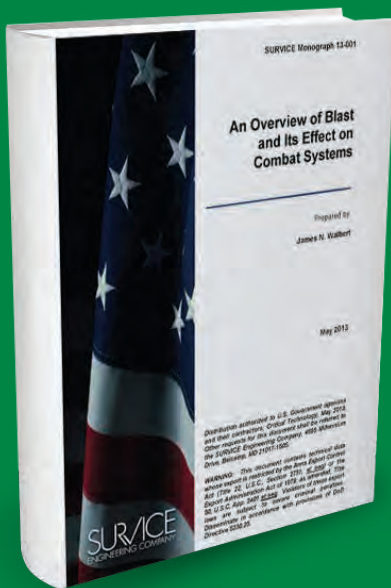
LOOK BEFORE YOU LEAP

Before you start your next R&D project, have DSIAC perform a free search of the vast repositories of previously performed Government-funded R&D. With access to nearly 1,300,000 digital records and almost 500,000 full-text documents, we can

provide tailored searches of both historical and the latest scientific and engineering information. New in this issue, we present the results of simple key word searches performed on the subject of each article; look for a breakdown of the results at the end of each article and see what you could be missing.

BOOK REVIEW

DSIAC is pleased to announce the availability of “An Overview of Blast and its Effect on Combat Systems” as the introductory edition of its Technical Monograph series. Each Technical Monograph is a one-volume work of research or literature on a single subject that is intended to capture unique (and potentially perishable) technical information, insights, and experiences from senior-level personnel and make them available to other community practitioners for the purpose of personnel/community development, technical training,



and/or information archiving. As such, Technical Monographs are often broader in scope and applicability, more detailed in content, and/or more closely reviewed/refereed than typical technical reports.

In “An Overview of Blast and its Effect on Combat Systems” the author discusses use of large explosive charges—whether in the form of military mines or improvised explosive devices (IEDs)—detonated under ground combat systems. Such explosive charges have long been a source of concern for those responsible for developing, analyzing, and improving these systems. And this concern has only increased in recent years as the use and size of these charges have markedly increased in modern combat zones. Unfortunately, while attempts to mitigate the effects of these charges on combat systems and their occupants have been widely reported in the media and elsewhere, the reports have often misrepresented the true physics and mechanics of the mitigation mechanisms. Thus, this monograph is intended to provide survivability analysts, designers, testers, and field assessors with a more complete understanding of the subject by

defining pertinent terminology, describing the fundamental physics of blast and other detonation products, examining various aspects of mitigation, and dispelling certain myths that surround these phenomena. In addition, Appendix A is included to discuss the effects on blast parameters of varying the type of specific energetic materials.

Please contact DSIAC to request a copy of “An Overview of Blast and its Effect on Combat Systems” Technical Monograph. Distribution is limited to U.S. Government agencies and their contractors and is subject to ITAR regulations. ■

BIOGRAPHY

JAMES WALBERT has approximately 40 years of survivability/vulnerability and related experience, including extensive and novel work as an interior and exterior ballisticsian, vulnerability/lethality tester and analyst, materials engineer, author, and instructor. His employers include the U.S. Army Material Testing Directorate, the U.S. Army Ballistic Research Laboratory (and its successor the U.S. Army Research Laboratory [ARL]), the Defense Advanced Research Projects Agency (DARPA), the SURVICE Engineering Company, and (currently) the Institute for Defense Analyses. He has authored/co-authored more than 50 technical publications, including the AIAA-published text *Fundamentals of Ground Combat System Ballistic Vulnerability/Lethality*, which was named ARL's Publication of the Year for 2009. Dr. Walbert also developed and teaches a highly acclaimed ballistic vulnerability/lethality course to Government and industry practitioners throughout the S/V community. He holds a B.S., M.S., and Ph.D. in mathematics from the University of Delaware and has taught mathematics and engineering at the University of Delaware, Penn State University, and Marymount University.

CONTRIBUTE AN ARTICLE TO THE DSIAC JOURNAL

The Defense Systems Information Analysis Center (DSIAC) publishes research and development (R&D) and engineering articles in a quarterly journal. The articles explore new ideas and emerging trends in science and engineering in nine focus areas: Advanced Materials; Autonomous Systems; Directed Energy; Energetics; Military

Sensing; Non-Lethal Weapons; Reliability, Maintainability, Quality, Supportability, and Interoperability (RMQSI); Survivability & Vulnerability; and Weapon Systems. The goal of the DSIAC Journal is to help researchers, engineers, and technical managers by providing a forum in which to share their expertise and lessons learned throughout the community and minimize redundant research. We publish original and high-quality

papers with the objective of covering the latest developments in the fields of engineering and/or technologies. All papers are published in print and electronic form and are indexed and cataloged in the DTIC R&D gateway.

For more information on contributing an article visit our website at <https://www.dsiac.org/resources/Journals/policy/dsiac-journal-article-submission-instructions>. ▶

CARBON NANOTUBES:

SMALL STRUCTURES WITH BIG PROMISE

By Paul Wagner

The unique physical, electrical, and molecular properties of carbon nanotubes (CNTs) cause them to be the focus of research for a wide range of applications. While commercial application for CNT technology is a central driver for much of this research, the Defense industry is also investing heavily in CNT research initiatives and manufacturers. And the technology is already finding its way into several military applications. This article explores ways in which CNT technology is currently being applied in products geared for the U.S. military, as well as some of the more promising future applications.

Even some “commercial” applications of CNTs have directly or indirectly benefitted the Warfighter.

CNTs, illustrated in Figure 1, are tiny (1 nm in diameter for single-walled tubes) molecules of pure carbon. They were accidentally discovered in the 1950s by Roger Bacon of Union Carbide while he was studying carbon at its triple point (the temperature and pressure at which an element can exist in a stable form as a solid, liquid, and gas). The tiny hollow tubes of carbon that he observed appeared to have a similar regular spacing as that seen in planar graphite [1].

The discovery remained a curiosity until the mid-1980s when a microscopist discovered

the spherical molecular structure illustrated in Figure 2. The spheres were dubbed “buckyballs” due to their similarity to the geodesic domes made famous by Buckminster Fuller.

It was soon realized that buckyballs were one of an entire class of carbon molecules now named *fullerenes*, which include the hollow tubes Bacon had observed. Each carbon atom in a fullerene molecule bonds with three other carbon atoms, and the molecule has exactly 12 pentagonal faces, although fullerenes can have a differing number of hexagonal faces. CNTs are fullerenes that have a hollow tubular structure; they can exist as single-walled carbon nanotubes (SWCNT) or multi-walled carbon nanotubes (MWCNT) forms.

Being pure carbon and of a near-defect-free molecular structure, an SWNT is normally 1 nm in diameter, yet it has the highest tensile strength of any known material. With CNT's specific strength approximately 200 times greater than that of steel, and yet 5 times the elasticity of steel at only 50% of the density of aluminum, these mechanical properties alone would cause CNTs to be of great interest to structural designers, offering the potential for immense strength with low mass.

Depending upon how the CNT atoms are aligned, the CNT can act either as an electrically conductive metal or as a semiconductor. As conductors, CNTs can provide 1,000 times the current-carrying capacity (per equivalent mass) as copper. CNTs also exhibit optical and thermal conduction properties that can be exploited for various applications. Doping, where certain impurities are introduced into the structure, allows specialized CNTs to function as highly specific and sensitive chemical sensors.

While new applications for CNTs continually arise, the primary reason that CNTs have not yet fully lived up to their potential is the difficulty in manufacturing them with the "right" properties for the desired application. With both the Defense and public sector industries investing heavily into CNT research, however, it is fully expected that manufacturing process innovations will help to solve the manufacturability issues.

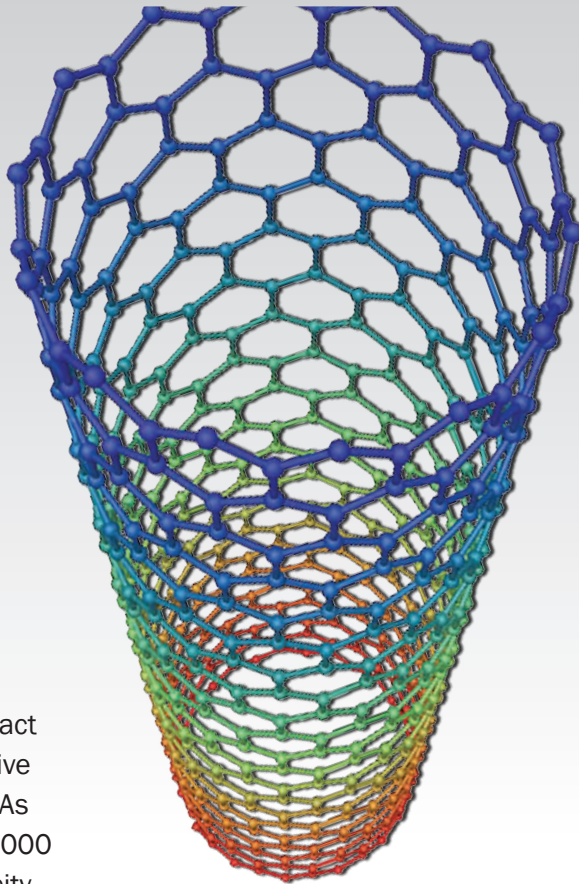


Figure 1: Single-walled "Zig-Zig" Carbon Nanotube.

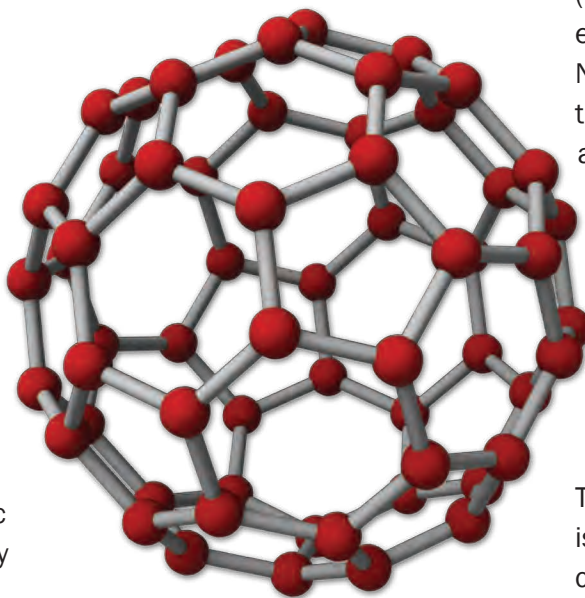


Figure 2: C-60 Buckyball.

Companies such as Nanocomp Technologies, Inc., a partner of the Department of Defense (DoD), is currently one of the leading manufacturers of CNT-based materials.

ARMOR

A likely use of CNTs for the military market will be lightweight body armor, as pictured in Figure 3. SWCNTs exhibit an extremely high elastic modulus and a high strain at tensile failure. These properties give them an energy absorption capacity 10 times greater than the fiber materials normally used in soft body armor. Not surprisingly, CNT fibers have already found their way into soft armor products such as the ones manufactured by AR500, Block Textiles, Amendment II, and NanoRidge (and their customer Riley Solutions, Inc. [RSI]). In fact, the product made by NanoRidge/RSI was chosen by the Defense Advanced Research Projects Agency (DARPA) to undergo testing and evaluation. Yet another company, Nanocomp, has been working with the U.S. Army to develop similar armor using Nanocomp's exclusive processes. With the use of CNT fibers, along with other materials such as Kevlar, thinner and lighter body armor can provide protection from level IIIA threats and blunt trauma, and it can be used in conjunction with hard armor [2, 3].

The aforementioned hard armor is typically manufactured from a ceramic such as silicon carbide or alumina. Although ceramics are quite hard, they are also brittle. Experimentation has shown that by

adding just 4% (by volume) of CNT fibers to alumina, the fracturing toughness can be increased by up to 94%. Composites of liquid crystal polymers with CNTs could also be cast or molded into armor plates and helmets [2].

Clearly, CNTs have multiple applications in armor and are seen as a vital technology that can improve the ability of armor to sustain ballistic energies, while at the same time decrease the weight of such armor. The weight reduction is vital for reducing Warfighter fatigue and increasing mobility, while also improving the mobility and fuel efficiencies of armored vehicles.

CHEMICAL AND BIOLOGICAL WEAPON PROTECTION

A team led by Lawrence Livermore National Laboratory (LLNL) and funded by the Defense Threat Reduction Agency (DTRA) is pursuing a variation on personal protective equipment for the military. Current-day chemical and biological protective suits are passive solutions that are heavy, bulky, and fully sealed. They are not amenable to the wearer's comfort, and tend to induce heat stress and fatigue. To address these issues, LLNL's Dynamic Multifunctional Material for a Second Skin Project is developing the CNT-based fabric, pictured in Figure 4, that will have the ability to repel either chemical or biological agents that may be dispersed by enemy combatants. The lightweight base CNT material provides permeability, as the pores

created by the CNTs facilitate gas transport that is several orders of magnitude greater than pores of any other material. The CNTs would be modified by "functional group" materials that will have the capability to quickly and automatically detect and react to various agents, reversibly switching from a highly permeable mode to a protective mode, sealing off chemicals, but allowing for sufficient "breathability."



Figure 3 (top): CNT-Based Body Armor.
Figure 4 (bottom): Experimental Chemical Protection Material.

The layered protective membrane would either close off the CNT pores or shed contaminated layers. It is anticipated that such suits could be deployed as early as 2022 [4].

In a parallel effort, scientists at the National Institute of Standards and Technology (NIST) are developing their own CNT-based materials that they believe have the potential to degrade certain chemical nerve agent weapons, such as sarin, tabun, and soman. The CNTs in the fabric are manufactured of a carboxylic group (COOH) reacted with copper chloride. The copper atoms serve to degrade the nerve agent molecules. While still early in the development phase, if successful, the fabric could be used to manufacture protective clothing for use in chemical "hot" zones [5].

A somewhat related application has researchers at the Massachusetts Institute of Technology (MIT) working on the development of a family of CNT-based chemical sensors. Led by professor Michael Strano and funded by MIT's Institute for Soldier Nanotechnologies, the first set of sensors developed makes use of the natural fluorescence properties of CNT. Coupling the CNTs with molecules that could bind to specific "target" molecules such as Sarin or other toxic agents, the sensor reaction causes the fluorescence to increase or diminish in the presence of the agent, providing an indication of the presence of the specific toxin. In another of their applications, the CNTs are coated with peptides normally found in bee venom, known as *bombolitin*s, resulting in a sensor that is reactive to nitro-aromatics, which are used in explosives, such as TNT. The reaction causes a shift in the wavelength of the CNT's fluorescence. By using an array of CNTs coated with different

bombolitins that react to molecules of different agents, it should become possible to identify the type of explosive. The CNTs could also detect the breakdown of such explosives as the materials degrade

[6]. MIT's next step in their sensor development is to integrate the sensor into a collection and analysis apparatus.

STRUCTURAL COMPOSITES

Composites are commonly used in manned and unmanned aircraft structures. However, to provide sufficient protection from lightning, as well as providing electromagnetic interference (EMI)/radio frequency interference (RFI) shielding, metallic meshes are often added as a layer (or layers) within the composite. These add weight, which reduce mission time and payload capability and/or increase fuel requirements. Applied NanoStructured Solutions (ANS), a subsidiary of Lockheed Martin, has developed infused carbon nanostructure (CNS) materials and processes that allow MWCNTs to be infused with materials such as glass, carbon, or ceramic fibers to produce customized composites that can be used in a variety of applications, including military aircraft structures [7]. Aside from allowing for reduced weight and improved structural strength, the MWCNTs used in the process are highly entangled, allowing the composite material to

act as a Faraday cage, protecting the structure from lightning strikes while providing EMI and RFI shielding. The CNT's conductive properties also facilitate health monitoring of the structure's integrity. In addition,

Scientists at NIST are developing their own CNT-based materials that they believe have the potential to degrade certain chemical nerve agent weapons, such as sarin, tabun, and soman.

the CNS materials of ANS can be used to replace the braiding or shielding used on electrical cables in virtually any application, providing superior shielding while reducing the weight by 30% or more. Reducing the weight, while at the same time providing a more robust solution through the use of CNS materials, positively affects mission time, payload capability, fuel savings, reliability, and longevity. Moreover, for portable devices, reduced-weight helps mitigate human fatigue.

The U.S. Army Research Laboratory is investigating CNT-based composites for helicopter rotor blades, but for a somewhat different reason. Presently in helicopter design, there is a trade-off between the stability of the aircraft and the amount of vibration transferred from the blades to the aircraft. That is, a stable design tends to transfer a significant amount of vibration to the aircraft, and vibration is one of the primary causes of excessive maintenance and repair. Ideally, it would be desirable to dampen the vibrations without adding extra weight or jeopardizing stability. Rotor

blades manufactured from a CNT composite may provide the answer. The CNT-based blades are expected to dampen vibration energy through the friction within the CNT matrix in a composite of carbon fibers.

Dissipating vibration in the blades would improve stability while lessening the amount of vibration that is transferred

to the aircraft—and without adding weight. The result should be an aircraft, such as the Apache pictured in Figure 5, that is capable of supporting increased payloads, better fuel efficiency, higher speeds, and lower maintenance costs. The CNT-based blade designs could be ready for fielding in the next generation of the fleet [8].

CAMOUFLAGE

A few of the more exotic applications for CNTs involve the exploitation of their thermoacoustic abilities.



Figure 5: AH-16 Apache: Greater Payloads and Faster Speeds with CNT-Based Rotor Blades.

Last decade, Chinese scientists discovered that a thin-film sheet of CNTs exhibit a thermoacoustic property; by applying a varying electrical signal to the sheet CNTs, the CNTs heat the surrounding air in reaction to the electrical signal, where the heated air generates a sound wave. Dr. Ali Aliev of the University of Texas proposed that the Navy could exploit this phenomenon by using CNT “speakers” to enhance sonar systems, while submarines could also use the speakers as noise cancellers, making the submarines more difficult for the enemy to detect and locate [9]. However, in a quite different application, Dr. Aliev demonstrated how the thermoacoustic effects of the CNT sheet can be used a cloaking mechanism; the heated air essentially creates a mirage effect, bending light around objects, causing them to be “invisible.” It has been speculated for some time that the U.S. military has been working on, and has demonstrated, what they say is a nanotechnology-based cloaking technique. Whether this technique is based on the CNT phenomenon demonstrated by Dr. Aliev has not been confirmed.

Further, a research team at the University of Waterloo invented (patent pending) another means of camouflage based on CNTs. The team’s CNT “paint” exploits the anti-reflective property of layered CNTs, which can absorb light in the spectrum spanning 0.2 to 200 μm , covering both the visible and infrared (IR) ranges. The flexible coating can be applied to virtually

any surface, including textiles, and is thermally and chemically stable. Because CNTs quickly reach thermal equilibrium with their environment, a coated object quickly adapts to the local background temperature, rendering the object “invisible” even to most night vision-equipped personnel [10].

ENERGY EFFICIENCY

The Power and Energy Strategy White Paper [11], prepared by the U.S. Army Capabilities Integration Center in 2010, outlined the increasing importance of energy to the base, the Warfighters, and their vehicles. An example of the concerns included in the paper is that of battery usage. Presently for a 72-hr mission, the average Warfighter carries about 70 batteries of 7 different types, weighing a total of approximately 16 lbs. The paper suggests a number of initiatives that should be pursued to address this and other aspects of power and energy, including a need for:

- Increased Energy Efficiency
- Decreased Weight of Energy Devices
- Innovative, Integrated Electrical Power/Energy Solutions, Ranging from Charging to Energy Harvesting.

CNTs can play a number of important roles toward achieving several of the Army’s goals. CNTs are proposed for use in a range of small primary and secondary batteries. At the anodes of lithium ion batteries, the high surface area afforded by CNTs increases the capacity and deliverable current and promises

improved lifetime. These advantages should allow for a decrease in the number and weight of the battery load required per Warfighter. CNTs are also being investigated for use in lead-acid batteries, leading to longer life in standard vehicles, thereby decreasing maintenance. And as the Military Services transition part of their vehicle fleet to electric or hybrid power, high-capacity lithium ion batteries with CNT anodes will serve to increase the operating and service life of CNT battery cells [12].

Super-capacitors based on CNT technology are also being investigated as a lower-cost, lower-weight alternative to some of the batteries used by the Warfighter. If successful, these would enjoy a much longer cycle life than can presently be attained by rechargeable lithium ion cells.

Additionally, solar cells, whether used in the field or in fixed installations, are an important means of generating electrical power and reducing the reliance on fossil fuels. Solar arrays, tents, and battery chargers are presently in use in the field by the military. The use of a CNT coating on solar cells or thermal devices, such as the device pictured in Figure 6, can increase their efficiency by reducing reflected light/heat, thereby capturing and producing energy more efficiently [13].

The Warfighter’s increasing dependence upon electronics to provide more (and more powerful) functionality to the array of gear he/she must carry leads to a



Figure 6: CNT-Based Solar Cells Promise Greater Conversion Efficiency.

demand for increased electronic processing power and memory requirements. To provide the functionality, yet in more compact packaging, the military is ultimately reliant upon advancements made in the commercial world of electronics to reap the benefits of high integration. Since the 1960s, the electronic industry has, more or less, abided by Moore's Law (the doubling of transistor density occurs every 18 months) when it comes to scaling of traditional, silicon-based devices. With today's high-end devices approaching the atomic limits of traditional silicon complementary metal oxide semiconductor (CMOS) devices, researchers are investigating non-silicon alternatives to keep pace with increased device density requirements. Not surprisingly, the size and the electrical (and thermal) properties of CNTs cause them to be a center of research into the next generation of electronics technology. CNT-based transistors have been in research since the 1990s. CNT-based transistors offer the potential of extremely small transistor

dimensions and high-speed operation, as well as reduced power consumption vs. silicon alternatives [14, 15]. While significant progress has been made in the past decade toward the manufacture of CNT-based transistors, much more work is required before they will be commercially viable.

CONCLUSION

Seldom has a single technology held so much promise as does CNT, and in such a wide array of applications, many of which are targeted for, or directly beneficial to, the military. Whether they are used to improve protective gear, structural apparatus, energy efficiency, or other applications not documented in this article, CNTs offer the promise of increased safety and effectiveness of our Service personnel. ■

BIOGRAPHY

PAUL WAGNER is a senior engineer for Quanterion Solutions Incorporated. He has more than 30 years of experience as a circuit and systems design engineer and as a product development director in the fields of telecommunications and fiber optic equipment. Mr. Wagner has a B.S. in Electrical Engineering from the University of Buffalo.

REFERENCES

- [1] AZoNano. "Carbon Nanotubes and Buckytubes - The Complete What, When, How, Why and Applications." <http://www.azonano.com/article.aspx?ArticleID=1597>.
- [2] Y. R. Mahajan. "Pursuit of the Ultimate Body Armor." Nanotech Insights, Centre for Knowledge Management of Nanoscience & Technology, July 2010.
- [3] Peter Wray. "Carbon Nanotube Fibers Woven for Military Armor." <http://ceramics.org/ceramic-tech-today/international/carbon-nanotube-fibers-woven-for-military-armor>, the American Ceramics Society, December 2010.
- [4] Anne M. Stark. "New Military Apparel Repels Chemical and Biological Agents." <https://www.llnl.gov/news/newsreleases/2012/Oct/NR-12-10-06.html>.
- [5] Global Security Newswire. "Researchers Develop New Fabric That Protects Against Chemical Weapons." <http://www.defenseone.com/technology/2014/05/researchers-develop-new-fabric-protects-against-chemical-weapons/84058/>, accessed, July 2014.
- [6] Anne Trafton. "Finding a needle in a haystack." <http://newsoffice.mit.edu/2011/explosive-detection-0510>, accessed July 2014.

[7] Lockheed Martin Corporation. "Infused Carbon Nanostructures." <http://lockheedmartin.com/content/dam/lockheed/data/corporate/documents/nano/materials-m.pdf>, accessed July 2014.

[8] T'Jae Gibson. "Army Researchers Chase Helicopter Performance Gains." http://www.army.mil/article/105134/Army_researchers_chase_helicopter_performance_gains/, accessed July 2014.

[9] American Chemical Society, "Submarines could use new nanotube technology for sonar and stealth." <http://www.sciencedaily.com/releases/2010/07/100714121743.htm>, Accessed July 2014.

[10] University of Waterloo. "Carbon Nanotube Coating for Visible and IR Camouflage." <https://uwaterloo.ca/research/waterloo-commercialization-office-watco/business-opportunities-industry/carbon-nanotube-coating-visible-and-ir-camouflage>, accessed July 2014.

[11] U.S. Army Capabilities and Integration Center. "Power and Energy Strategy White Paper." Research, Development and Engineering Command – Deputy Chief of Staff, G-4, 1 April 2010.

[12] Bill Scanlon. "New Research Bolsters Batteries with Nanotubes." National Renewable Energy Laboratory, http://www.nrel.gov/news/features/feature_detail.cfm?feature_id=13370, June 2014.

[13] Alex Saltarin. "MIT Develops Hot Carbon Nanotubes that Lets Solar Panels Draw More Sun." Tech Times, <http://www.techtimes.com/articles/2813/20140120/mit-develops-hot-carbon-nanotubes-that-lets-solar-panels-draw-more-sun.htm>, January 2014.

[14] Sebastian Anthony. "IBM Creates 9nm Carbon Nanotube Transistor that Outperforms Silicon." <http://www.extremetech.com/computing/115657-ibm-creates-9nm-carbon-nanotube-transistor-outperforms-silicon>, 2012.

[15] Tom Abate. "A First: Stanford Engineers Build Basic Computer Using Carbon Nanotubes." news.stanford.edu/news/2013/september/carbon-nanotube-computer-092513.html, September 2013.

ARTICLE SEARCH TERMS:

Carbon Nanotubes CNT Research
Development Trends Applications

RESULTS: 1,500

- Carbon Nanotubes (334)
- Electrical & Electronic Equipment (289)
- Nanotechnology (254)
- Composite Materials (175)
- Laminates & Composite Materials (171)
- Nanostructures (161)
- Foreign Reports (157)
- SBIR (Small Business Innovation Research) (148)
- Polymers (139)

*See page 3 for explanation ▶

SYNTHETIC APERTURE SONAR



IMPROVED TECHNOLOGY FOR IMPROVED MINE HUNTING

By Brett Israel and
Jennifer Weaver Tate

Over the last 60 years, sea mines (such as those pictured in Figure 1) have reportedly been responsible for damaging or sinking four times more U.S. Navy ships than any other weapon system [1]. Furthermore, next-generation mines, in addition to becoming more readily available, are increasingly sophisticated and difficult to find. Such mines can actually pinpoint the



Figure 1: Sea Mines, a Little-Publicized but Extremely Dangerous Threat.

size and shape of a ship moving in water; they can be fitted with acoustic, magnetic, seismic, and pressure sensors to detect a ship's approach; and they can determine the most effective time to detonate. In spite of these capabilities, few people outside the mine-countermeasure community seem to be discussing the threat posed by advanced sea mines. The subject tends to fall beneath the discussions regarding missiles, torpedoes, and other high-tech weapons—at least until a mine goes off.

However, such discussions may be changing. Ongoing sonar research being performed in part by the Georgia Tech Research Institute (GTRI) is promising to improve the Navy's ability to find sea mines deep under water. The underlying technology for this research—known as synthetic aperture sonar (SAS)—uses advanced computing and signal processing to create fine-resolution

images of the sea floor based on reflected sound waves.

SAS: NEW PROMISE FOR AN OLD TECHNOLOGY

Synthetic aperture technology originated in the radar community in the mid-20th century and was adapted by the sonar community approximately 20 years later. For many years, SAS was not practical for underwater use due to limitations associated with enabling technologies. As these technologies have advanced, researchers are reexamining the fielding of SAS systems for a wide range of commercial and military applications, especially mine detection.

Thanks to the long-term vision and a series of focused efforts funded by the Office of Naval Research (ONR) that date back to the 1970s, SAS is becoming an increasingly robust technology. And when it transitions

SAS is becoming an increasingly robust technology that is expected to dramatically improve the countermine mission.

to the fleet, the technology is expected to dramatically improve “the Navy’s ability to carry out the mine-countermeasure mission.

“The Navy wants to find sea mines,” said Daniel Cook, a GTRI senior research engineer. “There are systems that do this now, but compared to SAS, the existing technology is crude.”

The ONR-funded SAS research is being conducted in collaboration with the Applied Research Laboratory at The Pennsylvania State University. Researchers are making strides in improving the ability to predict and understand sonar image quality and are publishing and presenting results of their work at numerous conferences.

Sonar systems emit sound waves and collect data on the echoes to gather information on underwater objects. The Navy uses torpedo-shaped autonomous underwater vehicles (AUVs) (such as the AUV pictured in Figure 2) to map swaths of the sea floor with sonar sensors. One of the most well-known AUVs is the Bluefin 21, which was recently used to search for Malaysia Airlines Flight 370 after it disappeared in March 2014. AUVs zigzag back and



Figure 2: REMUS 600 AUV, Used to Map Sea Floor with Sonar Sensors.

forth in a “lawn-mowing” pattern and can map at a range of depths from 100 m to 6,000 m.

SAS VS. RAS

SAS is a form of side-scanning radar, which sends pings to the port and starboard sides of the AUV and records the echoes. After canvassing the entire area, data collected by the sensor are processed into a mosaic that provides a complete picture of that area of the sea floor to detect underwater objects, such as the WWII airplane pictured in Figure 3. SAS has better resolution than real aperture sonar (RAS), which is currently the most widespread form of side-scan sonar in use. RAS transmits pings, receives echoes, and then generates a corresponding strip of pixels on a computer screen. The sonar then repeats this pattern until it has an image of the sea floor. This technology is readily available and relatively inexpensive, but its resolution over long ranges is insufficient to suit the Navy’s mine-hunting needs.

Additionally, RAS sensors emit relatively high acoustic frequencies that are quickly absorbed by the seawater. SAS uses lower-frequency acoustics that can travel farther underwater, thus increasing the range at which fine-resolution pictures can be produced.

“RAS can give you a great looking picture, but it can only see out 30 to 50 m,” Mr. Cook said. “For the same resolution, SAS can see out to 300 m.”

Unlike RAS, SAS does not create a line-by-line picture of the sea floor. Instead, SAS repeatedly pings while recording the echoes on a hard drive



Figure 3: SAS-Produced Image of a Submerged Plane.

for post-processing. After an AUV surfaces, the hard drive is removed and data are analyzed by computers in a complex signal processing effort. The processing converts the pings into a large, fine-resolution image of the sea floor. The commonly accepted measure for fine resolution is a 1-inch by 1-inch pixel size, which can be achieved by SAS.

CONTRAST PREDICTION: A GAME OF SHADOWS

Tests of SAS in AUVs have produced fine-resolution images of sunken ships, aircraft, and pipelines. However, when looking at an image of the sea floor from above, operators sometimes have difficulty discerning the identity of simple objects. For example, certain mines have a circular cross section. When looking at a top-down image, an operator might not be able to tell the difference between a mine and a discarded tire. So, to discern if a circular-shaped object is a threat, operators also often consider the shadow that an object casts in the sonar image. Shadows cast by mines are often easy to distinguish from ones cast by clutter objects, such as tires. Accordingly, shadow contrast research is also used to help ensure that this distinction is as clear as possible.

“Predicting contrast has been a challenging problem for the sonar community,” Mr. Cook said. “We developed a compact model that allows us to compute contrast very quickly.”

Improving contrast prediction promises to have a ripple effect in mine-hunting capability. Naval

officers will be better able to plan missions by predicting how good the shadows will be in certain environments, which can lead to improved imagery, power conservation, and better performance for automatic target recognition software.

CONCLUSION

The problem of sea mines is not a problem that is expected to go away any time soon, especially as both mine and mine-countermeasure technologies continue to advance. Thus, it is a problem that the community must continue to address.

“Mines are a terrible problem,” said Mr. Cook. “They lie in wait on the sea floor, so you want to go find them with as few people in the process as possible—which is why we’re driven toward these autonomous vehicles with synthetic aperture sonar.”

The United States plans to replace its fleet of minesweepers over the next 12 years with multi-function vehicles outfitted with the latest mine-countermeasure capabilities. The ONR’s Commercial Technology Transition Office has made possible the transition of SAS into the Long-Term Mine Reconnaissance System (LMRS), an unmanned undersea vehicle that will enable submarines to extend their mine reconnaissance reach. It is hoped that efforts such as this, along with continuing research in the SAS arena, will go a long way toward advancing the community’s ability to detect and defeat the silent underwater threat of sea mines. ■

BIOGRAPHIES

BRETT ISRAEL is a communications officer at Georgia Tech in Atlanta, GA, where he covers topics related to biomedical engineering, chemical engineering, energy, and the environment. He works with national and international media outlets on coverage of Georgia Tech’s scientific research; helps train Georgia Tech faculty, staff, and students for media appearances; and travels with scientists to cover their expeditions. Prior to Georgia Tech, Mr. Israel was a senior editor at Environmental Health News, where he was a finalist for the Livingston Award for Young Journalists and won an Oakes Award Honorable Mention. He has B.S. in Biochemistry and Molecular Biology from the University of Georgia and an M.A. in Journalism from New York University’s Science, Health, and Environmental Reporting Program.

JENNIFER WEAVER TATE is a communications manager in the Electro-Optical Systems Laboratory (EOSL) at the Georgia Tech Research Institute in Atlanta, GA. She is responsible for reviewing, writing, and editing technical articles, reports, handbooks, newsletters, and promotional and advertising materials. She previously served as the Communications Manager of SENSAC and Managing Editor of Sensing Horizons. Ms. Tate attended Penn State and Tidewater Community College, majoring in Letters, Arts, and Sciences, and Business Administration, respectively.

REFERENCES

[1] Rabirot, Jon. “US Military Enters New Generation of Sea Mine Warfare.” *Stars and Stripes*, May 2011.

ARTICLE SEARCH TERMS:

Synthetic Aperture Sonar Mine Detection

RESULTS: 2,820

- Information Science (331)
- Acoustic Detection & Detectors (321)
- Symposia (292)
- Acoustics (284)
- Military Operations, Strategy, & Tactics (250)
- Foreign Reports (247)
- Administration & Management (254)
- Signal Processing (235)
- Defense Systems (215)
- Department of Defense (211)

***See page 3 for explanation ▶**

USING WEIBULL ANALYSIS TO GUIDE PREVENTIVE MAINTENANCE STRATEGY

By Richard Wisniewski, CRE

INTRODUCTION

As defined in NAVAIR 00-25-403, Reliability-Centered Maintenance (RCM) is “an analytical process to determine appropriate failure management strategies, including Preventive Maintenance and other actions that are warranted to ensure safe operation and cost-wise readiness” [1]. Similarly, NASA defines the purpose of RCM as “a process that is used to determine the most effective approach to maintenance. It involves identifying actions that, when taken, will reduce the probability of failure and which are the most cost-effective” [2].

Over the years, RCM has been used to achieve significant cost savings on a variety of programs. For example, RCM performed on the F-15 environmental control, fuel, landing gear, flight control, and oxygen and canopy systems resulted in 538 recommended changes to the maintenance procedures with an expected savings of \$21 million/year (450,000 manhours) [3]. Likewise, since 1997, shipboard fleet maintenance manhours have been reduced by nearly 50% through the implementation of RCM principles [3].

The objective of an effective RCM program is not to eliminate failures



but to reduce or mitigate the consequences of a failure when one occurs. The consequences of failure are usually assessed by their impact in the following four areas [4].

- Personnel and Equipment Safety
- Environmental Health/Compliance
- Operations (Availability)
- Economics.

One of the defining characteristics of RCM is *preventive maintenance (PM)*, which refers to actions performed periodically (or continuously) prior to functional failure to achieve the desired level of safety and reliability for an item. An effective RCM program strives to identify the PM necessary to ensure personnel safety, protect the equipment and environment, and ensure that the equipment will satisfy its operating requirements, and at a cost less than that of correcting the failure that the preventive task was trying to avoid.

PM tasks may be *condition-directed (CD)* or *time-directed (TD)*. A CD-PM task is a periodic diagnostic test or inspection designed to detect a potential failure condition prior to

functional failure. This detection is accomplished by comparing the existing material condition or performance of an item with established standards and taking further action accordingly. The objective of CD-PM is to maximize the useful life of each piece of equipment by allowing operation until a potential failure

maintenance planner must understand the time-dependent probability of failure of the targeted item relative to the expected life of the system. This article highlights how Weibull analysis can be used to analyze test or field-failure data to determine whether TD-PM is appropriate and, if so, determine the optimum replacement time.

The objective of an effective RCM program is not to eliminate failures but to reduce or mitigate the consequences of a failure when one occurs.

If warranted, Weibull analysis results can also be combined with cost data and reliability performance

requirements to determine the optimum maintenance time. is detected. A TD-PM task is one that is performed to restore or replace an item before it reaches an age at which the probability of failure significantly increases. The restoration or replacement occurs regardless of the item’s actual material condition. TD-PM tasks may be appropriate when a failure mode does not exhibit characteristics that demonstrate a detectable reduction in failure resistance or the PM interval (the time between potential failure indication and actual failure) is not long enough to permit a CD task.

requirements to determine the optimum maintenance time.

RCM AND PM

RCM requires a disciplined approach to maintenance. Because resources (hardware, test equipment, personnel, time, funding, etc.) are limited, PM for all functional failure modes is simply not affordable and, at times, not even advisable. As a result, PM must be prioritized so that operational risks are reduced to an acceptable level and so that cost efficiency in the maintenance process is achieved. One method of prioritizing PM is summarized in Table 1.

To determine the optimal time to schedule a TD-PM task, a

Table 1: PM Requirements for Various Failure Classes [5]

Failure Class	Class Description	PM Requirements
Critical Safety	Impacts operating safety where safety is related to loss of life and limb.	PM is <u>required</u> and must be able to reduce risk to an acceptable level. Otherwise, item must be redesigned. If redesign is not possible, identified risk must be expressly accepted.
Operating Capability	Failure that has a direct and adverse effect on operational capability (mission).	PM is <u>desired</u> if it is <u>effective</u> in reducing probability or operational consequences to an acceptable level.
Other Regular Functions	Failure that does not affect safety or mission capability. Typically these failures impact support functions.	PM is <u>desired</u> if it is <u>cost-effective</u> in reducing <u>corrective maintenance</u> .
Hidden or Infrequent Functions	Failures that impact functions that are not observable by operators during normal operation. They are characterized by an item for which there is no immediate indication of malfunction or failure.	PM is <u>required</u> to reduce the risk of multiple failures or function unavailability to an acceptable level.

The applicability of TD-PM is predicated on three fundamental assumptions: (1) the probability of failure of a new (or restored) item is less than that of the item currently installed; (2) the PM will reduce the probability of occurrence, unavailability or operational consequences to an acceptable level; and (3) the cost of performing PM will be less than the cost of correcting the failure after it occurs. PM will be ineffective for failures that are random in nature because a new item will be just as likely to fail as an in-service one. Even worse, PM would result in reliability degradation for failures that exhibit “infant mortality,” as a new item will be more likely to fail than an in-service one.

For PM to be desired, the probability of failure of a new item should be less than that of the original item. For example, if an item experiences an increased failure rate over time, but the degradation is so slow compared to the equipment operating life as to be insignificant, then PM would likely not be cost-effective. Likewise, if the risk or probability of failure is at an acceptable level, but the costs of PM and corrective maintenance (CM) are similar, then the lack of potential significant cost savings may result in a decision not to pursue PM. Ultimately, the decision to implement PM rests on the following:

- Reduced Safety Risk
- Reduce Impact on Operational Capability
- Economics.

To assess the effectiveness of

PM, a full understanding of the pertinent functional failure modes, failure causes, consequences and probability of failure prior to and after maintenance and the cost of preventive vs. corrective maintenance is necessary to ensure that limited resources are used efficiently.

One of the results of a Weibull analysis is an estimate of the percentage of a population that will have failed prior to a given period of time.

WEIBULL ANALYSIS APPROACH

Weibull analysis can be used to guide many of the decisions related to PM. One of the results of a Weibull analysis is an estimate of the percentage of a population that will have failed prior to a given period of time. This information is crucial for determining when an item should

proactively be restored or replaced. It can also be used to determine the optimal warranty period that minimizes customer dissatisfaction while preventing excessive replacement costs.

Four equations that describe the Weibull distribution and are necessary to determine the applicability of PM are shown in Table 2 [6].

Beta (β) is the Weibull shape parameter. It determines the shape of the Weibull distribution that best fits the data. It is the slope of the best fit line on the Weibull plot. Eta (η) is the Weibull scale parameter. Known also as an item’s *characteristic life*, it is defined as the time at which 63.2% of the population has failed. The variable “t” is the time at which the Weibull equations are to be evaluated.

The *hazard rate*, also known as the instantaneous failure rate, describes how the surviving members of a part population are failing at a given time. If the shape parameter (β) is less than 1, then the hazard rate is decreasing with time, and the item is said to be experiencing

Table 2: Weibull Distribution Equations Needed to Determine PM Applicability.

Description	Equation
Hazard Rate:	$h(t) = \frac{\beta}{\eta} \left(\frac{t}{\eta}\right)^{\beta-1}$
Probability Density Function (PDF):	$f(t) = \frac{\beta}{\eta} \left(\frac{t}{\eta}\right)^{\beta-1} e^{-\left(\frac{t}{\eta}\right)^\beta}$
Cumulative Density Function (CDF):	$F(t) = 1 - e^{-\left(\frac{t}{\eta}\right)^\beta}$
Reliability Function:	$R(t) = 1 - F(t) = e^{-\left(\frac{t}{\eta}\right)^\beta}$

infant mortality. In this case, PM would not be advisable because a new component would statistically be more likely to fail than one currently in service. If the shape parameter equals 1, then the hazard rate is constant and is equal to the reciprocal of the characteristic life. PM would not be advisable in this case because a new item would be just as likely to fail as one currently in service, given that it has survived up to that point. Because failures are randomly occurring, PM would not do anything to improve mission success but would negatively impact

availability and total maintenance cost. Consider, for example, the data provided in the Weibull plot shown in Figure 1.

In this case, the shape parameter is 1.027, indicating an exponential (or nearly exponential) distribution, with a resulting constant (or nearly constant) failure rate. The characteristic life is 3,423 hr. Using the following CM and PM data (MTTR_{corr} = 5 hr; MTTR_{prev} = 2 hr; CM cost = \$30,000; PM cost = \$5,000), the impact per unit of varying PM intervals on probability of failure, achieved availability, and total

maintenance cost over a 4,000-hr operating period is shown in Table 3.

As Table 3 indicates, although the probability of failure slightly decreases (69.1% reduced to 64.7%), the achieved availability is negatively affected by more frequent PM (99.9% reduced to 96%). Therefore, although the unit may fail slightly less often with more frequent PM, it will spend a greater percentage of its time out of service. Additionally, the total maintenance cost increases significantly with increasing frequency of PM, even though CM is more costly on a per unit basis. It is clear from this example that PM would not be recommended and the units should be allowed to operate to failure. If the probability of failure shown here is a safety or mission risk, redesign would be the preferred option because improvement in this area would not be possible through PM.

If the shape parameter is significantly greater than 1, then the equipment is likely experiencing wear-out. Thus, a new or restored item would be less likely to fail than one currently in service. Thus,

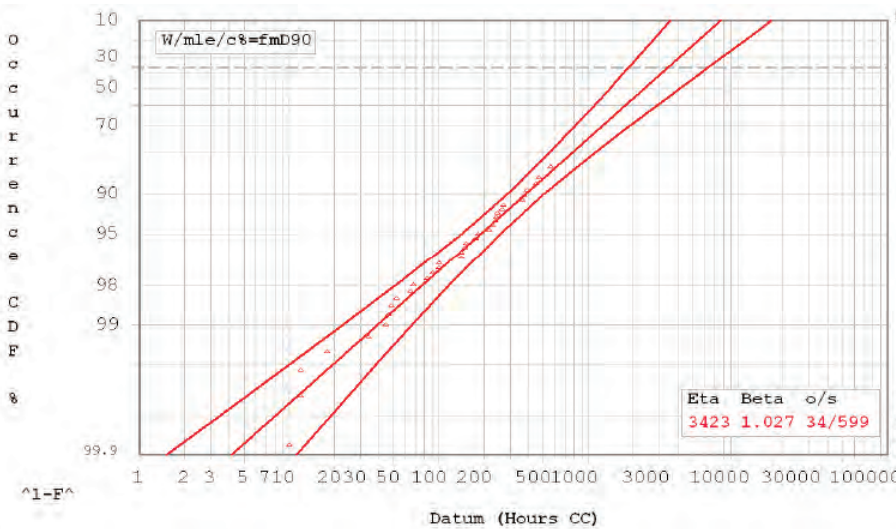


Figure 1: Weibull Data for a (Nearly) Exponential Case.

Table 3: Impact of PM on Probability of Failure, Achieved Availability, and Maintenance Cost ($\beta = 1.027$ case, $t = 4,000$ hr).

PM Interval	Probability of Failure @ 4,000 hr	CM Actions	PM Actions	Achieved Availability	CM Cost	PM Cost	Total Maintenance Cost per Unit
None	0.691	1	0	0.999	\$30,000	\$0	\$30,000
2,000	0.684	1	2	0.999	\$30,000	\$10,000	\$40,000
1,000	0.677	1	4	0.997	\$30,000	\$20,000	\$50,000
500	0.670	1	8	0.995	\$30,000	\$40,000	\$70,000
400	0.668	1	10	0.994	\$30,000	\$50,000	\$80,000
200	0.661	1	20	0.989	\$30,000	\$100,000	\$130,000
100	0.654	1	40	0.979	\$30,000	\$200,000	\$230,000
50	0.647	1	80	0.960	\$30,000	\$400,000	\$430,000

PM may be beneficial in reducing the probability of failure and/or reducing maintenance costs. Safety and mission specifications, the relative cost of PM and CM, the steepness of the Weibull curve, and the magnitude of the characteristic life relative to the equipment life expectancy would be the factors that dictate whether (and with what frequency) PM should be applied.

Weibull plots

with steep slopes tend to have a more clearly defined region, where the increase in the probability of failure accelerates. If the equipment will be retired prior to this point, then PM may not be necessary, as failure would be highly unlikely. Alternatively, if the equipment will still be in service at this time, then PM may be scheduled to ensure that safety and mission specifications are satisfied. If the equipment is not safety- or mission-critical, economic failures may drive the decision.

The more gradual the slope of the Weibull curve, the more difficult it is to determine the course of action; but the same principles apply.

Consider the data provided in the Weibull plot shown in Figure 2. In this case, the shape parameter is 1.62, indicating that wear-out is occurring with an increasing failure rate. The characteristic life is 1,728 hours. Using the same CM and PM data as in the previous example, the impact per unit of varying PM intervals on probability of failure, achieved availability, and total maintenance cost over a 4,000-hr operating period is shown in Table 4.

As Table 4 indicates, the probability of failure is significantly impacted by PM (98% at 4,000 hr when operated to failure vs. 22.7% at 4,000 hr with PM being performed every 50 hr). On the other hand, the achieved availability is negatively affected by more frequent PM (99.7% reduced

less than 35% at 4,000 hr, then PM must be performed at least every 100 hr. If maximizing availability is the goal, then PM performed at intervals of 500 hr or greater would be recommended, with maximum availability being achieved at 2,000-hr intervals. If maintenance cost is to

be minimized, 500-hr interval would be recommended.

Finally, the expected length of service should

also be considered, as it will affect the conclusions. Table 5 shows the analysis results from the same data set as used in the previous example, except that the length of service is 600 hr.

As Table 5 suggests, as long as the probability of failure and availability requirements are satisfied, no PM would be recommended.

Understanding the underlying failure distribution of an item is critical in determining whether or not PM is appropriate, and at what interval.

to 96.2%). Therefore, although the unit is likely to fail significantly less often with more frequent PM, it will spend a greater percentage of its time out of service. If minimizing the probability of failure is the overriding concern, then an increased frequency of PM is recommended.

For example, if the item is required to have a probability of failure of

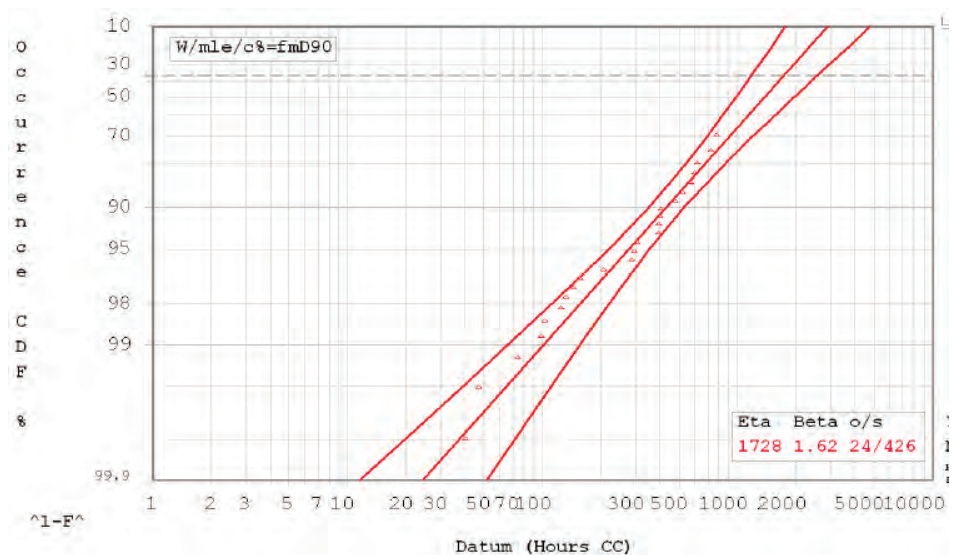


Figure 2: Weibull Data for a Wear-Out Case.

Table 4: Impact of PM on Probability of Failure, Achieved Availability, and Maintenance Cost ($\beta = 1.62$ case, $t = 4,000$ hr).

PM Interval	Probability of Failure @ 4,000 hr	CM Actions	PM Actions	Achieved Availability	CM Cost	PM Cost	Total Maintenance Cost per Unit
None	0.980	4	0	0.997	\$120,000	\$0	\$120,000
2,000	0.921	3	2	0.998	\$90,000	\$10,000	\$100,000
1,000	0.808	2	4	0.997	\$60,000	\$20,000	\$80,000
500	0.658	1	8	0.995	\$30,000	\$40,000	\$70,000
400	0.607	1	10	0.994	\$30,000	\$50,000	\$80,000
200	0.456	1	20	0.989	\$30,000	\$100,000	\$130,000
100	0.327	0	40	0.980	\$0	\$200,000	\$200,000
50	0.227	0	80	0.962	\$0	\$400,000	\$400,000

Table 5: Impact of PM on Probability of Failure, Achieved Availability, and Maintenance Cost ($\beta = 1.62$ case, $t=600$ hr).

PM Interval	Probability of Failure @ 600 hr	CM Actions	PM Actions	Achieved Availability	CM Cost	PM Cost	Total Maintenance Cost per Unit
None	0.165	0	0	0.997	\$0	\$0	\$0
300	0.111	0	2	0.993	\$0	\$10,000	\$10,000
200	0.087	0	3	0.990	\$0	\$15,000	\$15,000
100	0.058	0	6	0.980	\$0	\$30,000	\$30,000
50	0.038	0	12	0.962	\$0	\$60,000	\$60,000

SUMMARY

The discussion and examples presented in this article show how Weibull analysis can be used to guide TD-PM strategy. Understanding the underlying failure distribution of an item is critical in determining whether or not PM is appropriate, and at what interval. Equally important is the understanding of PM and CM times, preventive and corrective replacement costs, and equipment design life. Finally, a clear understanding of safety and mission reliability requirements is also necessary for an optimal PM program. ■

BIOGRAPHY

RICHARD WISNIEWSKI is a Senior Reliability Engineer at Quanterion Solutions Incorporated and has more than 28 years of experience in applying reliability and maintainability (R&M) and safety engineering methods and failure analysis/field support techniques on a variety of commercial/military systems, including radar, microwave/RF sensor systems, flight controls, mission computers, digital engine controls, and commercial and military hybrid electric vehicle drive train components. Mr. Wisniewski leads efforts to support government/industry customers in designing reliability/quality into products and systems, solve product reliability problems and identify corrective actions using electrical stress analyses, failure mode and effects analysis, root cause analysis, standard statistical analysis, and collection/analysis/modeling of failure data.

REFERENCES

- [1] NAVAIR 00-25-403. "Guidelines for the Naval Aviation Reliability-Centered Maintenance Process." Naval Air Systems Command, 01 July 2005.
- [2] "Reliability Centered Maintenance Guide for Facilities and Collateral Equipment." National Aeronautics and Space Administration, February 2000.
- [3] http://www.acq.osd.mil/log/mr/rcm/RCM_brochure.pdf.

[4] Wisniewski, R. "Quanterion RElease Series: Reliability Centered Maintenance." Quanterion Solutions Incorporated, 2013.

[5] S9081-AB-GIB-010. "Reliability-Centered Maintenance (RCM) Handbook." Revision 1, Naval Sea Systems Command, 18 April 2007.

[6] Lein, P. "Quanterion RElease Series: Weibull Analysis." Quanterion Solutions Incorporated, 2013.

ARTICLE SEARCH TERMS:

Weibull Analysis Preventive Maintenance

RESULTS: 1,310

- Reliability (202)
- Logistics, Military Facilities, & Supplies (110)
- Aircraft (93)
- Theses (89)
- Symposia (88)
- Maintenance (84)
- Mathematical Models (84)
- Maintainability (76)
- Administration & Management (74)
- Failure (69)

*See page 3 for explanation ▶

HIGH-POWER MICROWAVE

DIRECTED ENERGY WEAPONS:

A Model and Simulation Toolbox



U.S. Marine Corps

By John Tatum

INTRODUCTION

With continued advances in high-power radio frequency (HPRF)/microwave (HPM) directed energy weapon (DEW) technology, HPM DEWs are of increasing interest to the U.S. Departments of Defense (DoD) and Justice (DoJ). This increasing interest is based on numerous factors, including the ability of HPM DEWs to:

1. Provide the Warfighter/law enforcer with the ability to engage a target at the speed of light and produce scalable effects from temporary to permanent, thereby reducing the possibility of collateral damage.
2. Provide a relatively unlimited number of low-cost shots,

constrained only by the fuel supply of the HPM DEW's platform, which can greatly reduce the logistics tail and associated cost.

3. Leverage the development of all-electric ships, aircraft, and vehicles, which can provide the necessary prime power.

Additionally, while HPM DEWs are not likely to replace traditional kinetic energy weapons (KEWs) (such as guns, projectiles, and missiles) anytime in the near future, they have the ability to greatly enhance the effectiveness of KEWs by producing functional kills (or "soft kills") on certain targets, saving the limited KEWs for target destruction (or "hard kills").

This article briefly introduces some of the computer-based models/tools that are being used in the HPM DEW community to estimate

the effectiveness of these types of weapons against both adversary systems (for lethality analyses) and friendly systems (for survivability analyses).

PROBLEM

The power density/fluence required on a target to produce a functional kill depends not only on the target but also on the parameters of the HPM DEW, such as power, frequency/wavelength, modulation, and engagement angle. It is extremely time-consuming and expensive to test every target over a wide range of engagement angles and HPM DEW parameters. Accordingly, there is a significant need for computer-based modeling and simulation (M&S) that can be used to estimate the incident energy/power required on the target to produce an effect for a wide range of HPM DEW parameters.

Because the energy coupling to the target is stochastic in nature (due to both random and systematic uncertainties), in reality, we must estimate a target's probability of effect (P_e) as a function of the HPM DEW parameters, typically the incident power density/fluence on target. Further, we must ensure that the computer models are as realistic as possible. Therefore, they must undergo verification, validation, and accreditation (VV&A) to provide DoD engineers, testers, and program managers the ability to evaluate the potential effectiveness of an HPM DEW system.

HPM MODELS/TOOLS

HPM DEWs are similar in nature to a high-power radar transmitter with the exception that they can produce extremely high peak powers over tens of megawatts. An HPM DEW generates electromagnetic (EM) energy in the RF/microwave frequency range of roughly 1 to 35 GHz and uses an antenna to direct the energy to the target of interest. Because the HPM beam is typically much wider than a high-energy laser (HEL) or KEW, pointing and tracking is not as critical. Once the HPM energy hits a target, it can penetrate to the target's electronics via both intentional ports of entry (POEs) (i.e., front doors), such as an antenna, or through unintentional POEs (i.e., backdoors), such as cracks, seams, and cables. When the EM energy enters a target system, it reradiates inside and induces currents/voltages in the pins of the electronics that are sufficient to produce either a long-term electronic upset or permanent

damage. Additionally, because HPM DEWs can electronically attack a system with or without antennas and produce effects that last long after the energy is gone, DEWs represent a new form of electronic warfare (EW) known as an unconventional electronic attack (UEA).

Figure 1 illustrates a pyramid of models, with the base composed of physics and engineering models that are used to generate input to the next level of one-on-one engagement models. Because we are primarily interested in HPM DEW models that can be used to estimate the effectiveness of an HPM DEW against a selected target, these one-on-one engagement models are the models further discussed in this article.

HPM DEW ENGAGEMENT MODELS

Figure 2 illustrates the critical elements in a typical one-on-one HPM DEW engagement model. The model starts with a HPM source module that generates the energy and directs it toward the target. Next is the propagation module that takes into account the spreading loss of the beam as a function of range and atmospheric losses. The propagation losses for HPM in the frequency range of 1 to 35 GHz are typically not large unless the ranges are long (roughly tens of kilometers). Therefore, the propagation modeling for HPM is typically not as critical as it is for HEL DEWs, where the energy wavelengths are much shorter and can be greatly attenuated by the weather and atmospheric conditions.

DOD MODELING PYRAMID

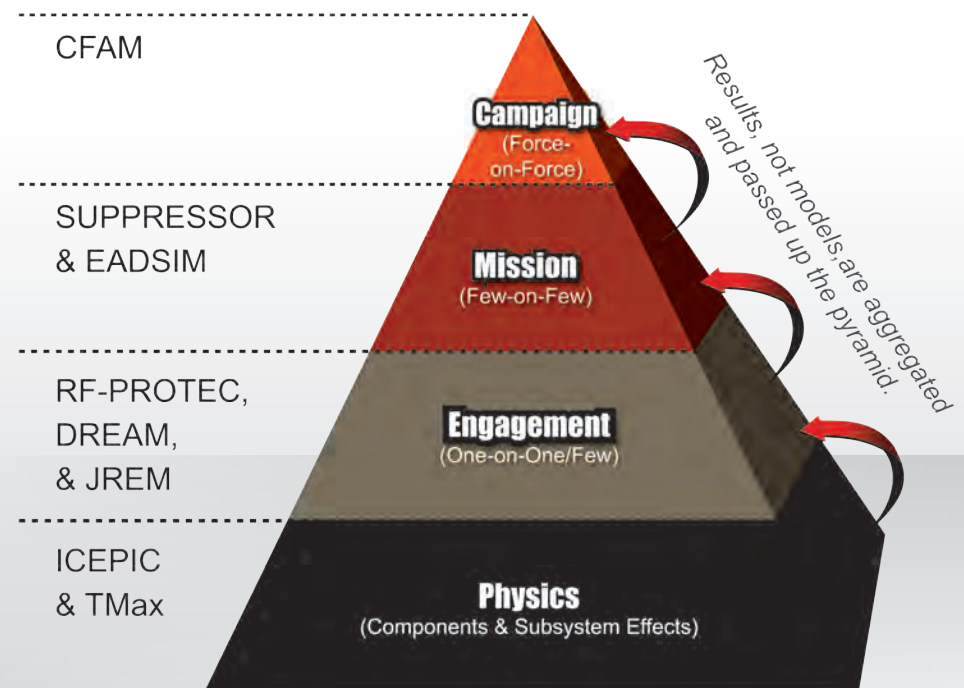


Figure 1: HPM Modeling and Simulation Pyramid with Examples of Existing Models.

Next in the engagement model we have the target interaction module or target vulnerability module. This module is where the target and its interior electronics are modeled. The target interaction module includes the RF coupling to the electronics and failure level of the electronics. If the power received by a

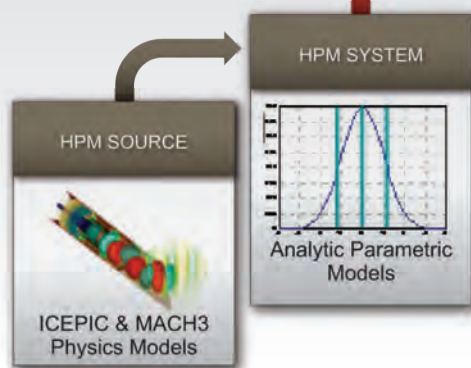


Figure 2: Modules for an End-to-End Simulation.

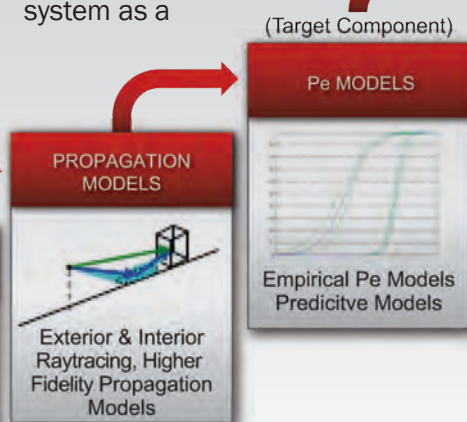
mission-critical component is greater than its failure level, we assume that the component fails and thus affects the target's function. Finally, we compute the overall probability of target failure by combining the failure levels of each of the critical components. The output of the engagement code is typically some form of P_e of the target as a function of the HPM power density on the target and/or associated range.

The following subsections discuss some of the HPM DEW engagement models that are used to evaluate the effectiveness of an HPM DEW concept.

Directed Radio Frequency Energy Assessment Model (DREAM)

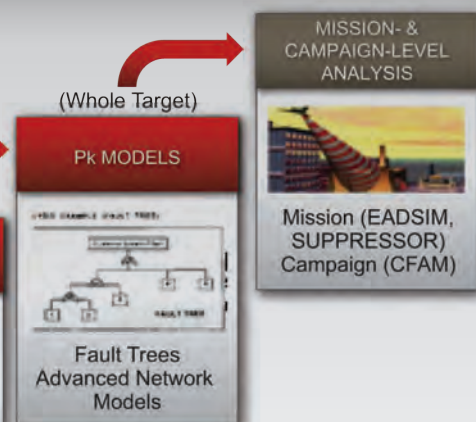
DREAM is a physics-based one-on-one engagement model developed by the U.S. Army Research

Laboratory (ARL) and SPARTA Inc. in the mid 1990s. It estimates the probability of electronic upset or damage to a target system as a



function of the HPM DEW's power density on target. The relatively easy-to-use standalone model is a computer implementation of the DoD Methodology for High-Power Microwave Susceptibility Assessments developed by the Office of the Secretary of Defense's HPM Effects panel in the 1980s. The methodology was based on the scientific method of performing pre-test analysis to predict the power densities required to produce target effects before exposing valuable electronic systems to pulses of HPM energy.

DREAM consists of two major submodules: the source module that generates the HPM pulses and directs them toward the target, and the target vulnerability module that computes the target's probability of electronic upset or damage. A DREAM user starts by selecting either the source icon or target icon on the graphical user interface (GUI). For example, if the source icon is selected, a source input box is displayed, requesting the



peak power of the HPM source, the frequency, the pulse width, and the pulse repetition rate. After completing this screen, the DREAM user selects the propagation or target icon. If the user chooses the propagation icon, the user is asked if he/she wants propagation in free space or if he/she wants to choose a weather condition, such as sunny or rain, as illustrated in Figure 3.

Next, the user selects the target icon, and a target screen appears to allow the user to represent the target in terms of a failure analysis logic tree (FALT). The tree shows the relationship of the mission-critical components to the function of the target. The user then tries to identify the most likely POEs on the target for the HPM to reach the critical component. For each of the critical components, the user selects the type of POE from a menu of typical POEs, such as aperture, dipole, etc.

The user then selects the type of electronic technology used for the mission-critical component, such as transistor-transistor logic (TTL), diodes, etc. Based on the frequency and the pulse width selected for the HPM source, DREAM computes the mean and standard deviation of the component failure distribution and the effective area of the POE.

DREAM then uses the POE area and the user-defined transmission loss for the entry path to compute the power received by the critical component. If the power received by the component is greater than the component's failure level, then DREAM assumes that the component fails. Finally, DREAM computes the target's overall P_e by combining all the failure levels of the critical components according to the target FALT.

DREAM has been distributed to several government agencies and their contractors and maintains a relatively large user community. It has been used by ARL to estimate pre-test predictions and to provide inputs to larger force-on-force models, such as the HPM Weapon Assessment Model in CASTFOREM. The Naval Air Warfare Center (NAWC) has also used DREAM to study the effectiveness of an airborne HPM weapon concepts against ship targets. To date, DREAM has been verified and validated through use, but not formally validated.

DREAM computes the P_e of a target based on the user input. Because it is essentially an "HPM-susceptibility-level calculator," the output (like that of any calculator) is only as accurate as the inputs used. A major weakness of DREAM is it assumes the user can identify the mission-critical component and the associated HPM paths to the component. For targets with front doors, it is a reasonable assumption that the user can identify the HPM entry paths since they are typically the same as the signal path. However, for targets with back doors, it is practically impossible to

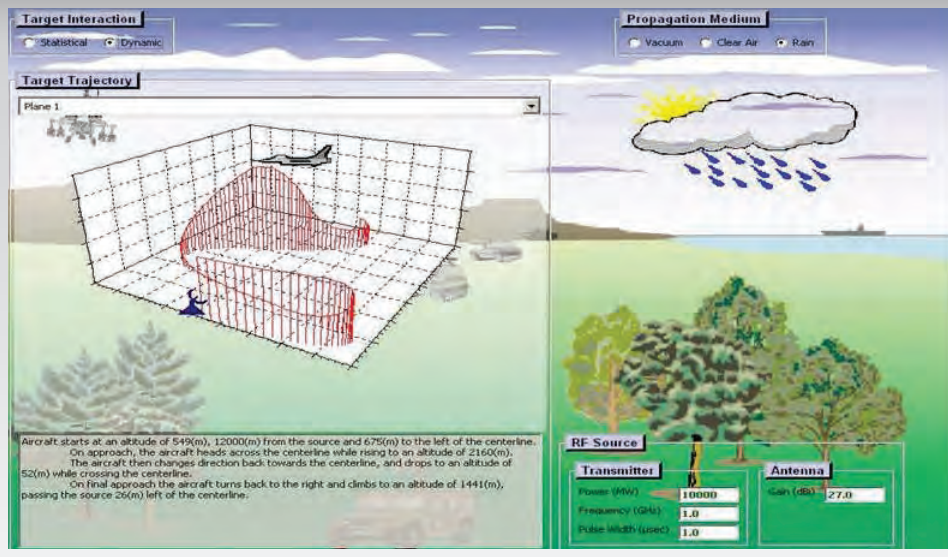


Figure 3: DREAM Input Screen Example.

ensure that one is modeling the correct entry path. To assist users, DREAM has an Operator's Guide that includes both a User and Analyst Guide [1]. The model is available from the U.S. Air Force Research Laboratory (AFRL).

RF Propagation and Target Effects Code (RF-PROTEC)

RF-PROTEC is a computer-based model that was developed by AFRL and ATK (now TechFlow) to estimate the effectiveness of an airborne HPM weapon against infrastructure targets (such as computer networks in a building) in terms of the probability of upsetting the network. RF-PROTEC consists of a source module, antenna module, propagation module and target interaction module, similar to DREAM. However, the model has a more sophisticated source and propagation module that uses Geometric Theory of Diffraction (GTD) to compute the electric fields/power density inside a target building and includes multiple path effects.

The target input to RF-PROTEC is experimentally derived P_e curves for each of the electronic systems in the target. The P_e curves are generated by exposing several electronic units to a fixed frequency and pulse width while increasing power density on the target to reach the upset/failure level. The fail and no-fail levels are combined to produce a P_e curve based on a logistic curve.

RF-PROTEC is an excellent model for simulating the generation and propagation of HPM energy to a target. However, the model requires several user inputs that make it less user friendly. To get an output from RF-PROTEC requires the user to have P_e curves for each of the electronic targets inside a structure. The source and propagation modules for RF-PROTEC have been verified and validated based on experimental data taken by AFRL on test buildings.

Joint RF Effectiveness Model (JREM)

JREM is a new one-on-one engagement model developed by AFRL and ARL and ATK (now

TechFlow). JREM runs on a personal computer and calculates the probability of kill (Pk) of target electronics as a function of an HPM DEW power and range. The model combines the best attributes of RF-PROTEC (the source and propagation module) and DREAM (the target vulnerability module) to allow a user to get an output with or without empirically based Pe curves for each of the target's subsystems. A JREM user can now use an empirical Pe curve if available or use the DREAM target vulnerability model to estimate a target probability of failure. JREM's source and propagation module has been verified and validated with experiments performed by AFRL. (Note: As mentioned previously, DREAM's vulnerability module has been verified but not formally validated.) JREM is available from AFRL [2].

HPM Lethality and Vulnerability Assessment (LAVA) Tool Kit

HPM LAVA is a new predictive modeling software tool to assess the effectiveness of HPM weapons on electronic systems of interest for blue-on-red or red-on-blue engagements. This tool is being developed for the Naval Air Warfare Center-Weapons Division (NAWC-WD) at China Lake by TechFlow and the SURVICE Engineering Company under a Phase II Small Business Innovation Research (SBIR) contract. HPM LAVA plugs into the validated JREM tool for modeling propagation of RF energy in complicated environments. It then uses a host

of statistical and deterministic cavity coupling algorithms to estimate the temporal and spectral characteristics of the HPM energy coupled into complicated enclosures. Finally, it leverages TechFlow's advancements in predictive circuit effects, garnered through several AFRL, Office of Naval Research, and Defense Threat Reduction Agency-funded programs, to model and predict the response of complicated electronics to the incident HPM stimulus. This tool captures the state-of-the-art advances in predictive HPM effects modeling backed by robust experimental data.

SUMMARY

With the ever-increasing use and development of HPM DEW technologies, the survivability/ lethality community's interest in, and use of, HPM DEW engagement models are expected to continue to increase. As described herein, the most promising of the models in current use/development are (1) DREAM, a standalone model that can be used to estimate the probability of electronic upset or damage as a function of the HPM power density on the target and associated range; (2) JREM, the latest HPM engagement model, which contains the best features of RF-PROTEC and DREAM; and (3) HPM LAVA, a developmental model that has the potential to provide more realistic HPM coupling modeling.

(Note: The AFRL Model POCs for DREAM and JREAM are Messrs. Tim Clark and Charles Davis). ■

BIOGRAPHY

JOHN TATUM is an electronic systems engineer with the SURVICE Engineering Company, working in the area of electronic warfare (EW) and radio frequency directed energy weapons (RF DEW). Previous to joining SURVICE, he worked for more than 36 years at the U.S. Army Research Laboratory's RF Electronics Division in radar/EW, where he directed and participated in electromagnetic (EM)/RF effects investigations on military systems and supporting infrastructure. Mr. Tatum investigated the feasibility and effectiveness of RF DEWs for various Army applications and served as the Army chairman of the RF DE JMEM Working Group. He also served as chair of the RF Effects Panel for the Office of the Secretary of Defense's Technology Panel on DEW. Mr. Tatum is a fellow of the Directed Energy Professional Society (DEPS). He has a B.S. in Electrical Engineering from the University of Maryland and has completed graduate courses in Communications and Radar at the University of Maryland and The John Hopkins University.

REFERENCES

[1] O'Connor, Robert, Karen McLaughlin, and John Tatum. "DREAM Operator's Manual." SPARTA Corporation and the U.S. Army Research Laboratory, 1995.

[2] Davis, Charles, and John Tatum. "Joint RF Effects Model Short Course." Presented at DE Systems Symposium, National Institute of Standards and Technology, Gaithersburg, MD, April 2012.

ARTICLE SEARCH TERMS:

Directed Energy Vulnerability Lethality
High-Powered Microwave RF DEW
Modeling Tools

RESULTS: 753

- Directed Energy Weapons (98)
- Administration & Management (92)
- Defense Systems (89)
- Military Operations, Strategy, & Tactics (84)
- Department of Defense (70)
- Export Control (70)
- Information Science (64)
- Countermeasures (62)
- Research Management (62)
- Antimissile Defense Systems (52)

***See page 3 for explanation ►**

BLAST DATA VISUALIZATION PART 1:

GENERATING 2D GRAPHS**WITH PYTHON**

By Will Woodham

**PYTHON: SLITHERING REPTILE OR POWERFUL VISUALIZATION TOOL?**

Human tendency is to avoid or even fear what we don't understand. All too often this avoidance/fear includes computer programming languages. And that's unfortunate because with even a little programming knowledge, one can perform some highly useful operations. Such is the case with Python and blast test data. The goal

of this article is to introduce some simple, yet powerful, Python code that will enable a user to transform that collection of test data he/she has tucked away on the hard drive into some full-color graphs. Admittedly, one could use a common spreadsheet tool to get some rudimentary-looking graphs, but why play in the sandbox when one can go to the beach? And nice-looking graphs are just the beginning. Learning Python can open up a whole new world of scientific computing

possibilities that can serve a user well in a variety of data analysis projects.

Before we dive into Python, let's look at some output examples. Figure 1 was produced by executing a simple Python program called *single_plot.py*. This snippet of code reads recorded acceleration data from a CSV (character-separated value) file and transforms the data into a plotted function. Additionally, the program calculates and displays the number

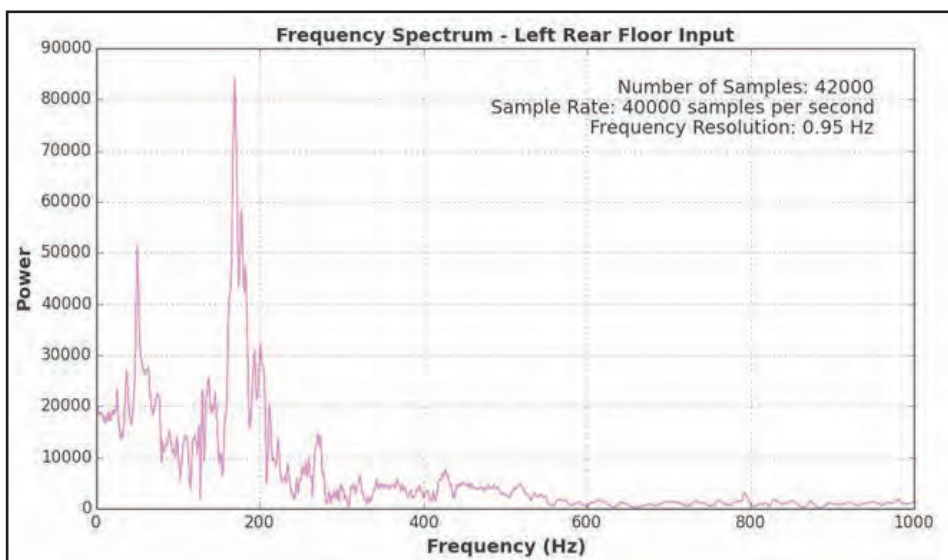
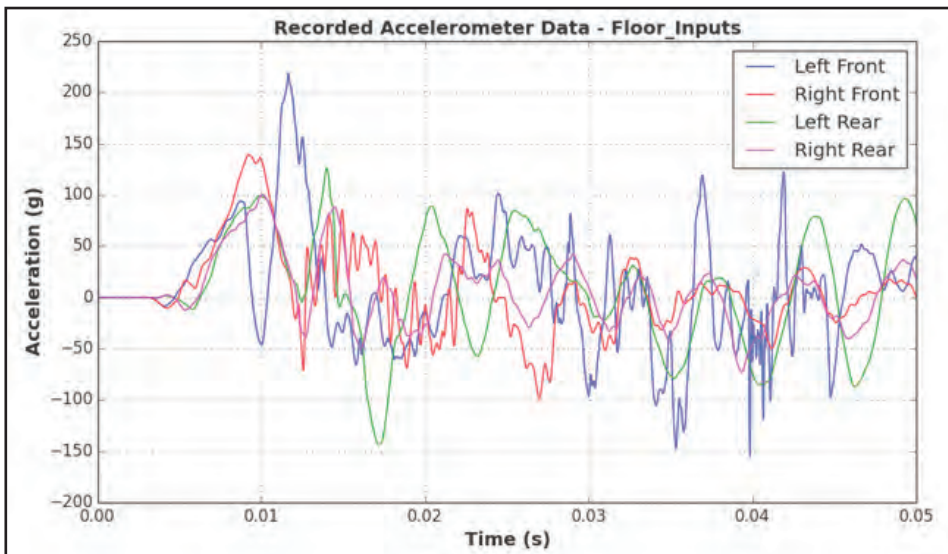
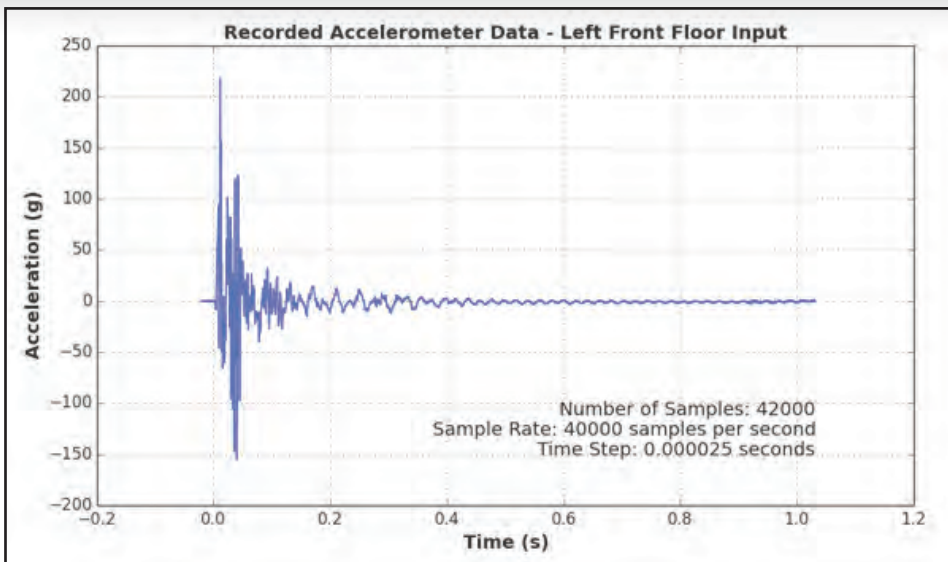


Figure 1 (top): Example of Acceleration Graph.

Figure 2 (middle): Graph of Multiple Acceleration Records.

Figure 3 (bottom): Frequency Spectrum Graph.

of samples in the data file as well as the sample rate and the time step.

As shown in Figure 2, multiple acceleration records can also easily be plotted on the same graph with *multi_plot.py*. This output provides a convenient way to compare results from different accelerometer locations. A legend identifies each of the color-coded records. And plot limit controls enable the user to produce a close-up view based on his/her desired time window.

As any good blast data analyst knows, a look at the time series data does not tell the whole story of the blast response. A frequency spectrum plot, such as that shown in Figure 3, provides the analyst with essential information about the frequency content of the data. This graph was produced by executing a Python program called *spectrum_plot.py*. Using the same data file as in Figure 1, the code reads and transforms the data from the time domain into the frequency domain to create the frequency spectrum graph shown. This program also calculates and displays the number of samples, the sample rate, and the frequency resolution.

SNAKE HANDLING FOR BEGINNERS

The first hurdle to overcome before one can unlock the power of Python is to download and install it locally. The good news is that it's free and easy to download (www.python.org ▶). Admittedly, sometimes the install can require a little patience; however, users should not be discouraged if they

get stuck. Chances are someone else has already encountered the same problem, so users experiencing installation difficulties should investigate the problem by searching the web. Once a user has installed Python, he/she will need to download and install the following modules to extend Python's capabilities for scientific computing, data visualization, and CSV file manipulation: *numpy*, *scipy*, *matplotlib*, and *csv*. Information regarding each of these applications is found at www.numpy.org, www.scipy.org, www.matplotlib.org, and <https://docs.python.org/2/py-modindex.html> respectively.

A NOTE ABOUT DATA FILES

Text files (.txt) and CSV files (.csv) are common test data file types. Text files can easily be converted into CSV files and vice versa using a common spreadsheet program or text editor. The Python programs described herein use a CSV file called *Floor_Inputs.csv*. The data in this file are arranged in rows and comma-delimited columns, as shown in the text editor screenshot in Figure 4. Reading the same file into a common spreadsheet program displays the data in separate columns based on the comma delimiter.

GETTING DOWN TO THE NITTY-GRITTY

Now that we've installed Python and the required modules, let's take a look at some code. One can find all three of the Python programs described in this article at www.piezopy.org under the

```
Floor_Inputs.csv
1 TIME (ms) , LF_Az (g) , RF_Az (g) , LR_Az (g) , RR_Az (g)
2 -20, 0.0181, 0.03518, 0.06013, 0.03712
3 -19.975, 0.08145, 0.03518, -0.01415, 0.03712
4 -19.95, -0.04525, 0.03518, -0.01415, 0.03712
5 -19.925, 0.08145, 0.03518, -0.08842, -0.02784
6 -19.9, 0.08145, -0.03198, -0.08842, -0.0928
7 -19.875, 0.0181, -0.03198, 0.06013, 0.03712
8 -19.85, 0.0181, 0.10235, -0.01415, -0.02784
9 -19.825, 0.1448, -0.09915, -0.01415, -0.02784
10 -19.8, 0.0181, 0.03518, 0.06013, 0.03712
11 -19.775, 0.08145, -0.03198, 0.06013, -0.15777
12 -19.75, 0.08145, -0.09915, -0.01415, 0.03712
13 -19.725, 0.08145, 0.10235, -0.01415, -0.02784
14 -19.7, -0.04525, -0.03198, 0.06013, 0.03712
15 -19.675, 0.08145, -0.09915, -0.08842, -0.0928
16 -19.65, 0.0181, 0.03518, -0.01415, -0.02784
```

```
1 #single_plot.py
2 """
3 A simple python program for reading and plotting a single
4 acceleration record from a csv file.
5
6 Requires Python (www.python.org) and the following python modules:
7 numpy, matplotlib, csv
8
9 Will Woodham
10 July 2014
11 woodhantech@gmail.com
12 """
13
14 #import python modules
15 import numpy as np
16 import matplotlib.pyplot as plt
17 import csv
18
```

Figure 4 (top): Property Formatted CSV Data File.
Figure 5 (bottom): The *single_plot.py* Program, Lines 1–17.

Code Snippets pull-down menu. Each of these can be copied and pasted into the user's favorite text editor and saved. Of course, the user will also need a CSV data file in the format (shown in Figure 4) with his/her acceleration data. Now let's take a look at *single_plot.py* starting at the top and working our way through the program a few lines at a time.

As shown in Figure 5, the top line contains the program filename. Note that anything with a # sign in front of it is a comment to help the user understand the program; it is not an executable part of the program. The next section, bounded by three repeating quote marks, contains a brief description of the program's

functionality along with authorship and version information. Lines 14–17 direct Python to use the modules listed to expand its capabilities.

As shown in Figure 6, lines 19–42 contain repeatable sections of code called *methods*. These subroutines act as small programs within a program. They receive input variables from the main program, perform a function based on that input, and return an output variable. The *single_plot.py* program has only three methods. The first method, starting at line 19, is called *samplecount*. This method counts the number of samples (rows) in a CSV data file. The resulting value is stored in a variable (*n*) and returned

```

18
19 #method to count number of samples in a data file
20 def samplecount(proj_folder,data_file):
21     with open(proj_folder+data_file, 'rb') as f:
22         reader = csv.reader(f)
23         row_count = sum(1 for row in reader)
24     n=row_count-1
25     return n
26
27 #method to construct a data array from a single column in a data file
28 def construct(proj_folder,data_file,col,n):
29     da = np.arange(0,n, dtype=float)
30     i=0
31     with open(proj_folder+data_file, 'rb') as f:
32         reader = csv.reader(f)
33         reader.next()
34         for row in reader:
35             np.put(da,[i], row[col])
36             i=i+1
37     return da
38
39 #method to calculate sample rate
40 def samplerate(n,t):
41     sr = int(n/(t.max()-t.min()))
42     return sr
43

```

```

43
44 #main program
45 def main():
46     #identify data file
47     proj_folder = 'C:/Users/will.woodham/Documents/PyData/blast/'
48     data_file = 'Floor_Inputs.csv'
49
50     #identify data columns
51     #Column 0 = Time (ms)
52     #Column 1 = LF Floor Az (g)
53     #Column 2 = RF Floor Az (g)
54     #Column 3 = LR Floor Az (g)
55     #Column 4 = RR Floor Az (g)
56
57     #creates a text label for each data column to be plotted
58     label = 'Left Front Floor Input'
59
60     #count number of samples
61     n=samplecount(proj_folder,data_file)
62
63     #read data and create arrays
64     t = construct(proj_folder,data_file,0,n)
65     Az = construct(proj_folder,data_file,1,n)
66
67     #convert ms to seconds (if necessary)
68     t = t/1000
69
70     #calculate sample rate
71     sr = float(samplerate(n,t))
72
73     #calculate time step
74     dt = float(1.0/sr)
75

```

Figure 6 (top): The *single_plot.py* Program, Lines 19–42.

Figure 7 (bottom): The *single_plot.py* Program, Lines 44–74.

to the main program. The value contained in n is then used in other methods, including the method, starting at line 27, called *construct*. This method reads the data from a single column in a CSV file and creates an array for that variable. Our example CSV data file contains five columns; column 0 for time and columns 1–4 for acceleration. In this case, *construct* is called twice in the main program, first to construct the time array (t) using data from column 0 and then again to construct the

acceleration array (Az) using data from column 1. The last method, starting at line 39, is for calculating the sample rate based on the number of samples (n) and the time array (t).

Now that we've addressed these important prerequisites, let's proceed to the main program. As shown in Figure 7, lines 46–48 identify the specific name and location of the CSV data file to be used. One will need to modify these lines for his/her particular case.

Lines 50–55 are a nonexecutable reference map of the data contained in the CSV file. This map also should be modified for the user's particular case, ensuring he/she has the correct variable and units for each data column. Line 58 creates a text label for the acceleration data that will be used later in the plot title. Line 61 is where the main program calls the *samplecount* method described previously and stores the number of samples in the variable (n). Lines 64 and 65 are calls to the *construct* method, where the time (t) and acceleration (Az) data arrays are created. Because the time data in our example CSV file is in units of milliseconds, we convert this to seconds by executing line 68. This conversion makes the sample rate calculation more straightforward. As described previously, line 71 is a call to the method *samplerate*, which stores the calculated value in the variable (sr). The time step or interval between samples (dt) is calculated on line 74.

Let's now look at the code that unleashes the powerful and versatile graphing capabilities of Python and Matplotlib. As shown in Figure 8, the rest of the program, beginning with line 73, is dedicated to transforming all the data we gathered and calculated into a customized full-color graph. This transformation includes both displaying the graph in an interactive window and storing a PNG (portable network graphics) format image file containing the graph for future use.

Line 77 creates an 11-inch-wide by 6-inch-tall figure in which to display the graph. Line 78 plots a blue curve representing the data

```

75
76 #plot the acceleration data within a figure
77 fig = plt.figure(figsize=(11,6))
78 plt.plot(t, Az, 'blue')
79 plt.grid()
80 plt.title('Recorded Accelerometer Data - '+label, fontsize=14, fontweight='bold')
81 plt.xlabel('Time (s)', fontsize=14, fontweight='bold')
82 plt.ylabel('Acceleration (g)', fontsize=14, fontweight='bold')
83
84 #print data stats on the graph
85 plt.text(t.max(), Az.min()+40, 'Number of Samples: '+str(n), horizontalalignment='right', fontsize=14)
86 plt.text(t.max(), Az.min()+20, 'Sample Rate: '+str(sr)+' samples per second', horizontalalignment='right', fontsize=14)
87 plt.text(t.max(), Az.min(), 'Time Step: %.6f seconds' % dt, horizontalalignment='right', fontsize=14)
88
89 #save the figure
90 fig.savefig(proj_folder+'Az_fig1.png')
91
92 #display the graph
93 plt.show()
94
95 if __name__ == '__main__':
96     main()

```

Figure 8: The *single_plot.py* Program, Lines 75–96.

for acceleration (Az) as a function of time (t) and stores it in the figure. Line 79 draws a grid with default grid spacing on the graph. Line 80 creates a title to go above the graph using the previously assigned data label. Line 81 specifies the label for the vertical axis while line 82 calls out the label for the horizontal axis. The user can customize items such as font size and font weight for these labels. Lines 84–87 use the *plt.text* function to print the number of samples (n), sample rate (sr), and time step (dt) directly on the graph in the lower right-hand corner. Line 90 saves the figure containing the graph to a PNG file with a specified path and filename. Finally, line 93 launches an interactive window and displays the figure within that window.

SEE SPOT RUN? GO SPOT GO!

To run *single_plot.py*, all a user needs to do (after Python and the required modules have been installed) is open a command window or console window, navigate to his/her project folder using the *cd* command, type *python single_plot.py*, and press Enter (as shown in Figure 9). Alternatively, one can

just right-click on *single_plot.py* in Windows Explorer and select Open with Python. The user just needs to remember to modify lines 47–58 to match his/her data file before running it.

An interactive window, such as the window shown in Figure 10, should appear on the screen. Using the window interface control buttons at the bottom left, one can manipulate the graph by zooming in and out,

panning, etc. A PNG image file of this same graph should also now be available for viewing in the user's specified project folder. When finished, a user can simply close the window and the program will terminate.

Now, let's take a look at the other two blast data visualization programs covered in this article.

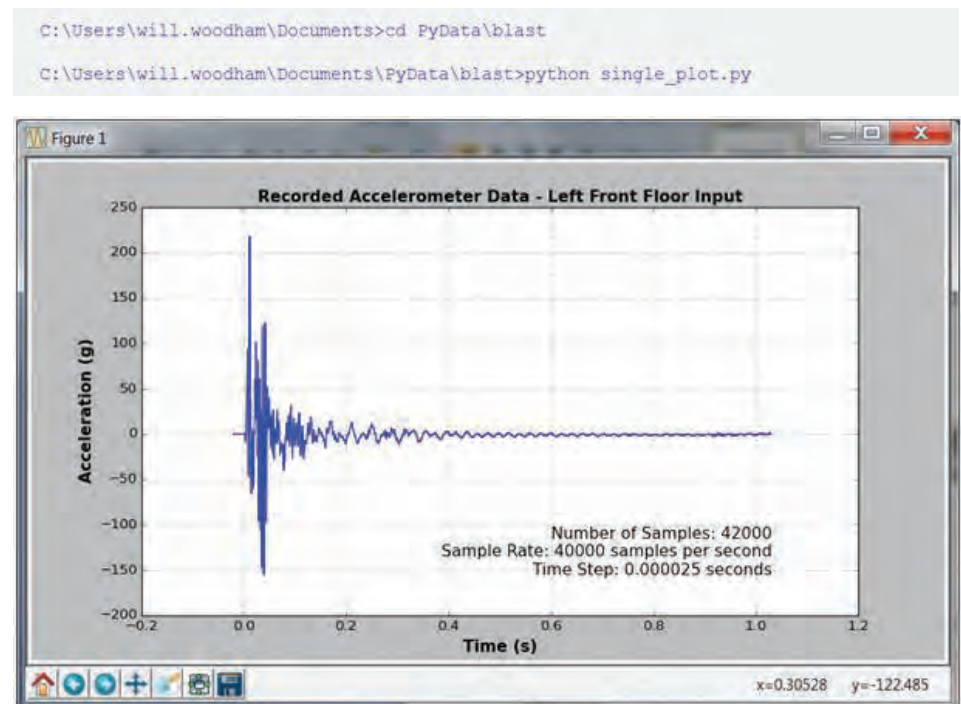


Figure 9 (top): Running *single_plot.py*.
Figure 10 (bottom): Interactive Window.

PYTHONIC THEME AND VARIATIONS

Because the basic structure of *multi_plot.py* is the same as *single_plot.py*, we only discuss what makes them different rather than rehash what we've already learned with *single_plot.py*.

As shown in Figure 11, on lines 69–72 of *multi_plot.py*, instead of constructing a single acceleration array, as in *single_plot.py*, arrays for all four acceleration records found in *Floor_Inputs.csv* are constructed. As the name implies, lines 85–89 of *multi_plot.py* plot all four acceleration records on a single graph. Line 86 prevents each of the plot commands from overwriting the previous one. To focus in on the first 50 ms of data, line 96 specifies the horizontal axis limit to be 0.050 s. And finally, Line 99 sets up a legend on the graph for identifying the four color-coded acceleration record plots. The rest of the program is the same as *single_plot.py* described previously.

AN ALTERNATE VIEW OF THE UNIVERSE

As humans, we are accustomed to viewing the world within the time domain. We don't naturally think about how things might look in the frequency domain. Moreover, as blast data analysts, we know that when it comes to evaluating the response of a structure to blast loading, the frequency domain is extremely important. A frequency spectrum graph provides us with an alternate view of the data that sheds light on the frequency content

```

66 #read data and create arrays
67 t = construct(proj_folder,data_file,0,n)
68 LF_Az = construct(proj_folder,data_file,1,n)
69 RF_Az = construct(proj_folder,data_file,2,n)
70 LR_Az = construct(proj_folder,data_file,3,n)
71 RR_Az = construct(proj_folder,data_file,4,n)
72
73
74 #convert ms to seconds (if necessary)
75 t = t/1000
76
77 #calculate sample rate
78 sr = float(samplerate(n,t))
79
80 #calculate time step
81 dt = float(1.0/sr)
82
83 #plot the acceleration data within a figure
84 fig = plt.figure(figsize=(11,6))
85 plt.plot(t, LF_Az, 'blue')
86 plt.hold(True)
87 plt.plot(t, RF_Az, 'red')
88 plt.plot(t, LR_Az, 'green')
89 plt.plot(t, RR_Az, 'magenta')
90 plt.grid()
91 plt.title('Recorded Accelerometer Data - '+label, fontsize=14, fontweight='bold')
92 plt.xlabel('Time (s)', fontsize=14, fontweight='bold')
93 plt.ylabel('Acceleration (g)', fontsize=14, fontweight='bold')
94
95 #set plot limits
96 plt.xlim(0,0.050)
97
98 #add a legend
99 plt.legend((LF_label, RF_label, LR_label, RR_label))
100

```

```

13
14 #import python modules
15 import numpy as np
16 import matplotlib.pyplot as plt
17 import csv
18 from scipy import signal
19 from scipy import fftpack
20

```

Figure 11 (top): The *multi_plot.py* Program, Lines 66–100.

Figure 12 (bottom): The *spectrum_plot.py* Program, Lines 13–20.

of the data and how that content is distributed. A frequency spectrum graph is a plotted function of relative power with respect to frequency. The higher the amplitude, the higher the relative power of that particular frequency in the data.

Frequency response analysis is a deep subject and deserves more attention than we can afford to provide it in this article. Having said this, let's stick to providing a way to visualize the data in the frequency domain and leave the frequency response discussion for another time. Although much different in the result, the structure of the *spectrum_plot.py* program is highly similar to *single_plot.py*. This similarity allows us to once again

focus on the differences rather than rehashing the parts that are the same.

As shown in Figure 12, the first difference we notice is that *spectrum_plot.py* requires additional module import commands on lines 18 and 19 to further expand Python's capabilities to do signal processing.

On lines 82 and 83 (of Figure 13) we see that power (p) and frequency (f) arrays are constructed using *fftpack* module commands. Lines 85–91 create a figure and plot the power (p) as a function of frequency (f) on the graph with corresponding grid, title, and axis labels. Lines 93–97 limit the range of frequency to be displayed on the graph. And finally,

```

80
81 #calculate fft
82 p = abs(fftpack.fft(Az))
83 f = abs(fftpack.fftfreq(n, dt))
84
85 #plot the frequency spectrum within a Figure
86 fig = plt.figure(figsize=(11,6))
87 plt.plot(f, p, 'violet')
88 plt.grid()
89 plt.title('Frequency Spectrum - '+label, fontsize=14, fontweight='bold')
90 plt.xlabel('Frequency (Hz)', fontsize=14, fontweight='bold')
91 plt.ylabel('Power', fontsize=14, fontweight='bold')
92
93 #set max frequency to be plotted
94 flim = sr/40 #frequency plot limit
95
96 #set plot limits
97 plt.xlim(0,flim)
98
99 #print data stats on the plot
100 plt.text(flim*0.95, p.max(), 'Number of Samples: '+str(n), horizontalalignment='right', fontsize=14)
101 plt.text(flim*0.95, p.max()-4000, 'Sample Rate: '+str(int(sr))+ ' samples per second', horizontalalignment='right', fontsize=14)
102 plt.text(flim*0.95, p.max()-8000, 'Frequency Resolution: %.2f Hz' % df, horizontalalignment='right', fontsize=14)
103

```

Figure 13: The `spectrum_plot.py` Program, Lines 80–103.

lines 99–102 print appropriate data statistics directly on the graph.

HUNGRY FOR MORE?

At this point, hopefully the user has a grasp of what's possible with a little programming knowledge, Python or otherwise. If the user is hungry for more, he/she won't want to miss the next article in this series, Blast Data Visualization Part 2: Generating 3D Animations with Python. We'll build upon the Python foundation

we've laid in Part 1 and delve into the wild and wonderful world of 3D animation. Happy slithering! ■

BIOGRAPHY

WILL WOODHAM is an employee of the SURVICE Engineering Company, supporting blast test data analysis for the U.S. Army Tank Automotive Research Development and Engineering Center. He has extensive experience in vehicle design and blast survivability analysis and is the author of a blog (at www.piezopy.org) advocating the development and use of open source software tools (such as Python) for blast data visualization and similar applications. Mr. Woodham holds a B.S. in Mechanical Engineering from the University of South Florida and an M.S. in Product Development from the University of Detroit Mercy.

ARTICLE SEARCH TERMS:

Blast Visualization Python
Survivability Vulnerability

RESULTS: 69

- Computer Programming & Software (15)
- Military Forces & Organizations (11)
- Medicine & Medical Research (9)
- Symposia (9)
- Computerized Simulation (8)
- Data Bases (8)
- Computer Programs (7)
- Space Warfare (7)
- Biology (6)
- Lethality (6)

***See page 3 for explanation ▶**

MODEL UPDATE

RADGUNS V2.4.3

On behalf of the National Ground Intelligence Center (NGIC), DSIAC announces the upcoming release of the Radar-Directed GUN System Simulation (RADGUNS) version 2.4.3, along with accompanying model documentation. The new version will be available from DSIAC starting in October 2014.

The RADGUNS model is used to evaluate the effectiveness of Air Defense Artillery (ADA) gun systems against penetrating aerial targets.

It is also used to evaluate the effectiveness of different airborne target characteristics (radar cross section [RCS], maneuvers, use of electronic countermeasures, etc.) against a specific ADA system. The model is a complete one-on-one simulation that includes the weapon system, operators, target model (RCS and presented/vulnerable-areas), flight profiles, environment (clutter and multipath), electronic attack, and endgame.

The release of RADGUNS 2.4.3 is the result of an extensive review, funded by the Joint Aircraft Survivability Program (JASP), of three RADGUNS gun systems. The review resulted

in seven software change requests, which are addressed in this release. Notable improvements to the model include:

- Updated documentation.
- A fix to the number of bullets fired when multiple gun systems are present.
- A corrected steering of multiple gun systems on a battery radius.
- An improved capability to accurately make fire control computer predictions for a single gun system offset from the radar.
- A corrected gain value issue in a receiver routine. ■

A PROMISING FUTURE FOR US NAVY **VERTICAL LAUNCHING SYSTEMS**

By Eric Fiore, CSEP

INTRODUCTION

F For the past 30 years, shipboard vertical missile launching systems have transformed naval warfare by providing continually evolving launch capability to respond to a myriad of theater-based threats. Unmatched in performance and flexibility, these systems have changed the way all navies think about sea-based missile systems. With the ability to simultaneously respond to multiple aerial, surface, and submerged threats, the vertical missile launching system has become the aspiration of navies around the globe.

And the future of vertical missile launching systems appears even brighter. Recent advances in ballistic missile defense technology have introduced a new and expanded role for the U.S. Navy's Vertical Launching System (VLS). With repeated successful intercepts of increasingly complex targets, the U.S.-developed Aegis Weapon System, which includes a radar, weapon control system, VLS, and several classes/families of missiles, has redefined maritime strategy. In addition to performing the traditional navy-specific missions of air, surface, and subsurface defense, many of the newer Aegis-equipped ships are being built or upgraded with

ballistic missile defense (BMD) capability. The Aegis BMD capability has proven so successful that it has even precipitated new U.S. BMD policy, including President Obama's recent decision to leverage Defense investments by adopting a phased adaptive approach to BMD [1]. This approach entails the hybridization of sea- and land-based missile defense systems built upon the Aegis system. This new land-based version of the Aegis has been branded with the moniker "Aegis Ashore."

This article provides a brief history of the U.S. Navy VLS followed by a "how it works" functional description of the system architecture. Industry efforts to leverage investments and further expand the capability of the VLS are also discussed. The article concludes with several thoughts for future research and development (R&D), including an idea that may offer additional life cycle cost reduction opportunities.

HISTORY

The concept for a ship-based vertical missile launching system was first conceived to support the air defense systems of U.S. Navy surface ships equipped with guided missiles. This concept involved designing a modular, below-the-deck system that would be capable of storing and launching an encanistered Standard Missile (SM), a key armament of the Aegis Weapon System. The below-the-deck design was envisioned to support a greater density of 360° hemispherical firepower with significantly reduced mechanical movement when compared with legacy rotating guide-arm

launchers, such as the system pictured in Figure 1. To this day, the advantages of maintaining a below-the-deck missile magazine and launching system have gained such widespread appeal that several domestic and international variants of the VLS concept exist to accommodate a variety of guided missiles of varying size and capability. The U.S. Navy designated the first U.S. surface ship VLS as the Mark (Mk) 41.



Figure 1: Rotating Guide-Arm Missile Launcher

The Mk 41 VLS was conceived to be built upon a standardized rectangular configuration. While the modular configuration allowed some degree of mission and hull design flexibility, the launchers were essentially designed as forward and aft centralized missile magazines, as pictured in the Ticonderoga-class

guided missile cruiser (CG) *USS Lake Champlain* (CG 57) of Figure 2. U.S. Navy CGs are large combat vessels that operate primarily in a Battle Force role. The ships are designed for multi-mission air, sea, submarine, and land warfare and typically support carrier battle groups and amphibious forces or operate independently or as flagships of surface action groups. CGs were designed to accommodate eight forward and aft modules, and each module was designed to accommodate missiles housed in environmentally sealed canisters. Under normal launch conditions, both the launchers and canisters are designed to be serviceable and reusable.

For air defense, the U.S. fleet is equipped with a Mk 41 VLS designed to support the launch of SMs. This capability continues to be upgraded, including the ability to launch new, improved variants of the SM and the Enhanced Sea Sparrow Missile (ESSM). The Vertically Launched Anti Submarine Rocket (ASROC or VLA) provides submarine defense. And for long-range land attack missions, the U.S. fleet is equipped



Figure 2: Ticonderoga Class Guided Missile Cruiser *USS Lake Champlain* (CG 57)

with Tomahawk-missile-launching capability. International variants of the Mk 41 VLS can have nearly identical capability but are generally configured to meet the specific needs of the respective international navy.

The Aegis Weapon System was fully integrated for sea-based operational testing and evaluation onboard the *USS Norton Sound* in the early 1980s. And in 1986, the *USS Bunker Hill* became the first commissioned ship in the

Ticonderoga class of U.S. Navy warships to receive the production version of the Mk 41 VLS. Today, modernized Ticonderoga-class warships maintain nearly comparable guided missile combat capability to the newer Arleigh Burke-class of guided missile destroyers, such as the *USS Milius* (DDG 69), pictured in Figure 6. As the primary Mk 41 VLS platforms for the U.S. Navy, each ship class was designed to serve evolving military roles with regard to vertical missile launch capability.

But in terms of maximum load-out, the CGs can support a maximum canister load of 122, compared to the 96 maximum canister load of the DDGs. In addition to serving the U.S. Navy, the Mk 41 VLS is also serving 12 other international navies on a variety of ship classes [2].

The basic foundation of the Mk 41 VLS is the eight-cell module, which can be installed in a ship in any desired number to meet specific mission and hull requirements.

REARMING AT SEA

The early Mk 41 VLS designs supported a requirement to be able to replenish expended missiles while out at sea. To facilitate this requirement, early MODs of the Mk 41 VLS included the collapsible and storable strike-down crane pictured in Figure 3. While spirited debates persist to this day regarding the necessity to replenish at sea, the crane was ultimately determined to be impractical and, in some instances, dangerous to use, especially with the larger and significantly heavier Strike canister of the Tomahawk Land Attack Missile (TLAM) and SM2 Blk IV missile. Consequently, the strike-down crane is no longer offered as

part of the system, and it continues to be removed from the Ticonderoga class ships.

There remains a common misconception that the reclaimed magazine space is available for additional missile launching capability, boosting CG missile storage capacity from 122 cells to 128. In fact, this perceived capability does not exist. When the strike-down crane is removed, the opening is simply sealed with a metal plate that is welded to the deck, as pictured in Figure 4 [3]. When a warship equipped with a Mk 41 VLS runs out of missiles, it returns to a port where expended canisters are removed and loaded canisters are installed with land-

based cranes, such as the operation pictured in Figure 5.

Since the inception of the Mk 41 VLS concept, the U.S. Navy has yet to become engaged in a sustained maritime conflict with an adversary of comparable or atypical capability that would have required replenishment at sea. And considering contemporary financial constraints, which could result in a decrease in the number of available guided missile ships and corresponding missiles on station, the debate may continue to linger a bit longer until the policy/strategy is ultimately tested (or changed) or until guided missiles simply become obsolete.



Figure 3: VLS Strike-Down Crane.



Figure 4: Removed VLS Crane.



Figure 5: Rearming the VLS.

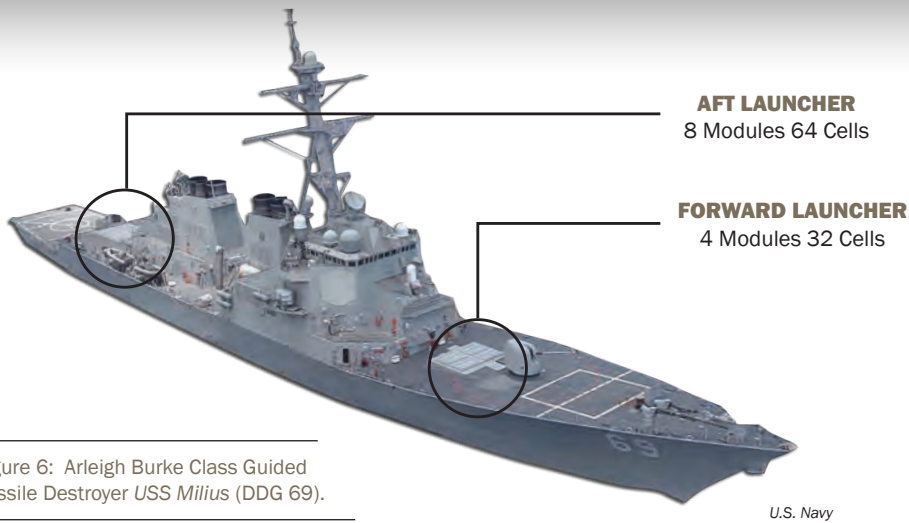


Figure 6: Arleigh Burke Class Guided Missile Destroyer *USS Milius* (DDG 69).

Mk 41 VLS is currently deployed in 13 different configurations, ranging from a single module to 16 modules. The basic module is currently available in two lengths: Strike and Tactical. The U.S. fleet employs the Strike module, which is approximately 25 ft (7.6 m) tall and capable of launching the largest SMs, such as those used to support sea-based, mid-course BMD and long-range tactical strike missiles, such as the Tomahawk. The Tactical module is approximately 22 ft (6.7 m) tall and capable of accommodating the same missile types as the Strike, with exception to the Tomahawk and SMs used for BMD [2]. Lockheed Martin no longer tenders the smaller 17-ft (5.2 m) Self-Defense module because it cannot accommodate the ESSM Block 2 [4].

A similarly configured international version of the U.S. VLS is the Sylver (SYstème de Lancement VERTical) designed by the French company Direction des Constructions Navales S.A. (DCNS). This launcher also comes in several variants, each designated by its height. The A-35 and A-43 VLSs were developed for

launching short-range surface-to-air missiles; the A-50 VLS was developed for the longer-range Principal Air Missile System (PAAMS); and the A-70 VLS was developed for larger missiles, such as a land attack cruise missile. The designation numbers refer to the approximate length (in decimeters) of the missile that can be accommodated. For example, the A-43 VLS can hold missiles that are up to 4.3 m long, while the A-70 VLS can accommodate missiles up to 7 m long [5].

Similar to the Mk 41 VLS, the Sylver VLS is configured in eight-cell rectangular modules, except for the A-35, which is also available in a four-cell module. The Sylver can also accommodate missiles that are quad-packed in a single cell or canister, much like the U.S. quad-packed ESSM. However, unlike the Mk 41 VLS, which uses a common plenum and uptake to expel rocket exhaust gas, the Sylver reportedly uses a cell-based modular composite uptake system [6]. The primary air defense weapon used by the Sylver VLS is the Aster missile, which is similar to the U.S. SM.

The U.S. Navy's next-generation multi-mission guided missile destroyer is the Zumwalt-class destroyer, pictured in Figure 7. The Zumwalt is also designated as a DDG but with the hull numbering system starting at 1000 (i.e., DDG 1000 is the first ship of the class). Designed with the latest technology, the Zumwalt-class destroyer uses a completely different VLS architecture and hot gas management system. Designated as the Mk 57 VLS, the launching system is configured around the periphery of the ship instead of in forward and aft centralized magazines, as is employed with the Mk 41 VLS on current CGs and DDGs.



Figure 7: Newest Class of U.S. Guided Missile Destroyers *USS Zumwalt* (DDG 1000).

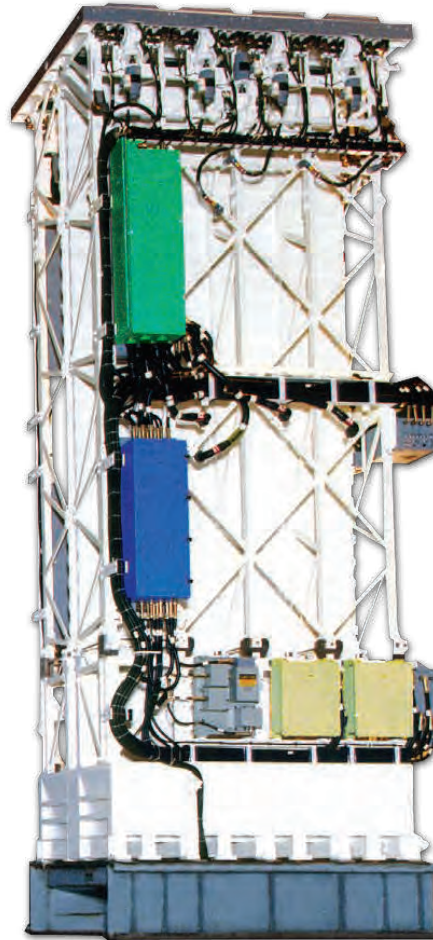
MK 41 SYSTEMS DESIGN

Since the mid-1980s, the Mk 41 VLS has maintained a consistent mechanical structure built around the eight-cell modular structure, while the system electronics have been continuously upgraded. The upgrades have incorporated new missile integration capabilities, mitigated obsolescence, and leveraged the benefits of commercial-off-the-shelf (COTS) components and open system

computing architectures, all with the goal of improving systems performance while reducing the systems life cycle cost. The primary system components of the Mk 41 VLS include two Launch Control Units (LCU), one to 16 eight-cell modules with respective module electronics, and encanistered missiles. For each launcher, forward or aft, and regardless of the number of installed modules (between one and eight), there are 400-Hz and 60-Hz power distribution units to supply power to the launcher electronics. Additional launcher support items (e.g., lights, phone, power receptacles, etc.), system transformers, and a Damage Control Junction Box (DCJB) are also provided. Outside the secured launcher area, there is a remote Launch Enable and Status Panel. The Mk 41 VLS also comes with an entire complement of ancillary equipment used for land-based and shipboard testing and maintenance.

The Baseline VII Mk 41 VLS, pictured in Figure 8, was purposefully designed to support a common modular architecture with a high degree of commonality and interchangeability. Any component of any launcher module can be interchanged with any other launcher module. This choice in architecture adds significant performance in operational availability, survivability, and versatility while minimizing staffing and training requirements. Because the system was designed to accept any missile in any cell, the Mk 41 VLS can simultaneously accommodate multiple weapon control systems (WCS) for the respective missiles of every

warfighting mission area—anti-air warfare (AAW), including ballistic missile defense, anti-submarine warfare (ASW), and anti-surface warfare (ASuW). Additionally, to facilitate fast response to multiple



Lockheed Martin

■ LESQ ■ MCP ■ PPS

Figure 8: Baseline VII Mk 41 VLS Module.

diverse threats, the Mk 41 VLS can simultaneously prepare one missile in each half of a launcher module and can also fire a four-missile salvo of ESSMs from one canister.

The functional allocation of the latest Mk 41 VLS design is illustrated in Figure 9. AAW, ASW, and ASuW

missions are initiated from their respective WCSs, where intent-to-launch commands are generated. These commands are routed to two LCUs located in two different Combat System Equipment Rooms (CSERs). During normal operations, each LCU controls half of the missile launchers in any ship. However, when in a causality mode, either of the LCUs can control all the launchers. Each LCU communicates with all WCSs. The LCUs are responsible for managing launch history, inventory, missile availability, and selection. Depending on the mission, when the LCU is commanded to select and fire a missile, the respective LCU selects the appropriate missile from launcher inventory and then coordinates launch activity with the Launch Sequencer (LSEQ) of the missile to be launched. The LSEQ checks for hazards and initiates the launch sequence. A typical launch sequence consists of checking for hazards; turning power supplies on and off; and energizing and operating relays, motor hatches, and plenum drains.

The VLS module, consists of an upright structure that provides vertical storage space for eight missile canisters. A deck and hatch assembly at the top of the module protects the encanistered missiles during deployments. Generally, the hatches are only opened to perform maintenance or to permit missile launches. The plenum and uptake structure capture and vent hot missile exhaust gases vertically up through the module to the atmosphere through the uptake system, as illustrated in Figure 10.

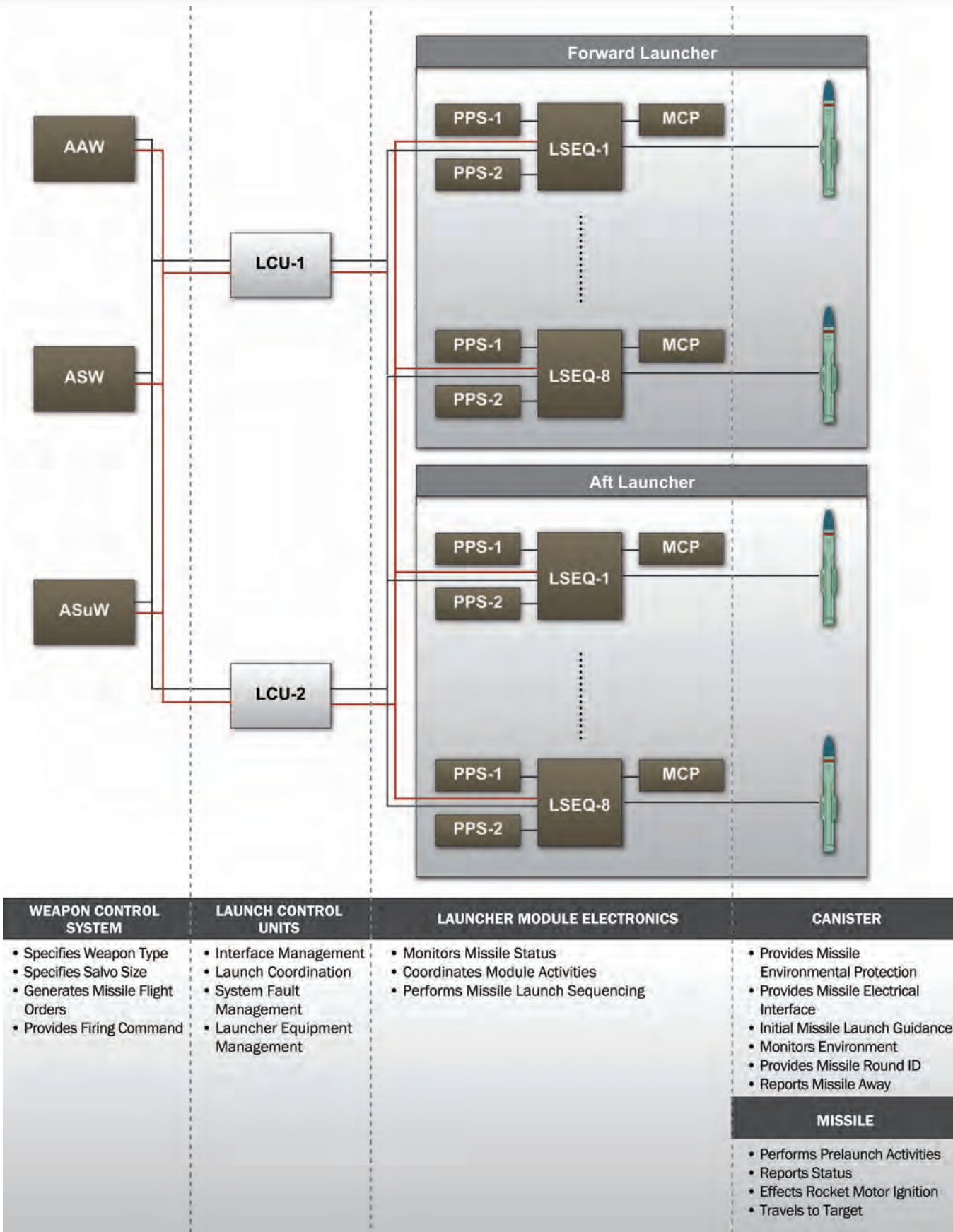


Figure 9: Functional Allocation of the Baseline VII Mk 41 VLS.

Electronic equipment mounted on the eight-cell module coordinates and performs the launch of missiles. The latest Mk 41 VLS design is designated as Baseline VII. For each module, the electronics consist of an LSEQ, Motor Control Panel (MCP), and two Programmable Power Supplies (PPS). Because the missiles are launched from centralized magazines, where missiles are stored inches apart, the management of rocket motor exhaust gas is critical for ship safety and launcher maintainability.

A Status Panel is located outside of the launcher magazine to receive and display the status of all launcher modules and all hazard signals from within the launcher. The panel also routes this information to the ship's command station. Most importantly, the Status Panel manages the launch enable command, which is required to enable the launch of a missile. Storage, shipping, and integration of weapons is facilitated with environmentally sealed and canisterized missiles. To support the requirement for long-term storage, the canisters are equipped with desiccant. The canisters are designed to accommodate the

variety of missiles illustrated in Figure 11. While the length of a missile can vary significantly, all canisters maintain a common 25-in square form factor with a common 145-pin electrical connector interface to the launcher. Forward and aft end covers provide

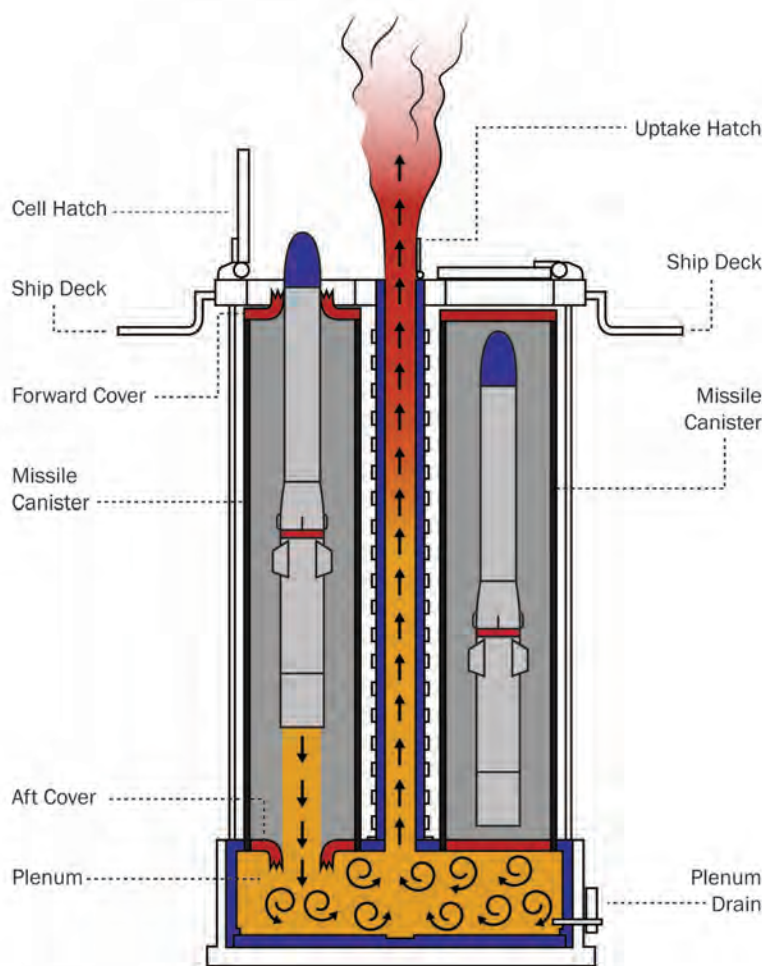


Figure 10: Mk 41 VLS Hot Gas Management System.

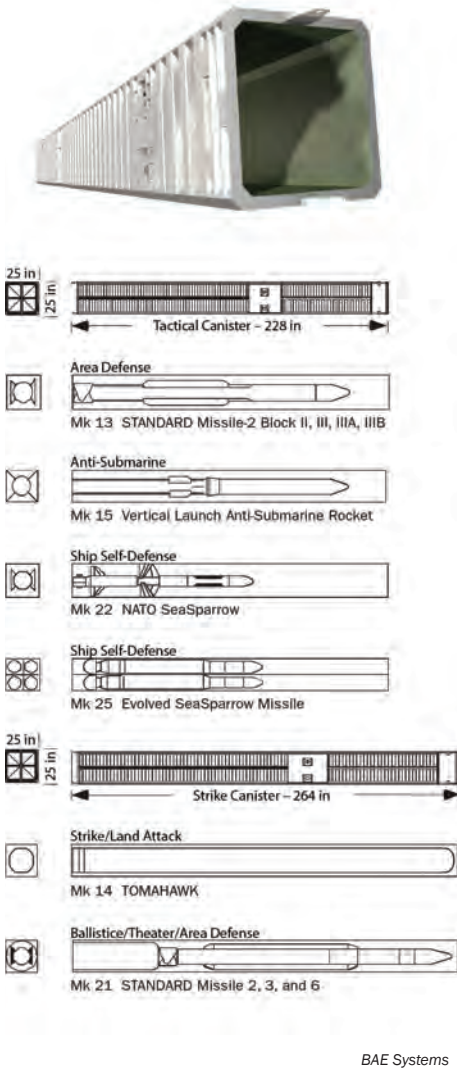
environmental seals for the missiles. The aft cover is ruptured at rocket motor ignition, which also generates an electrical signal to inform the weapon system that the rocket motor has in fact ignited. Almost immediately after rocket motor ignition, the restraint bolts are blown

and the missile begins to egress the canister by physically penetrating the forward cover. In the event the restraint bolts do not release the missile after rocket motor ignition, an overtemperature sensor confirms the restrained launch and activates a water deluge of the canister. The

deluge system pumps fresh water into the canister to cool the system, and if the temperature does not decrease sufficiently, the system continues to pump in sea water until it does. The water is removed from the launcher module plenum via a controlled drain.

The more recently designed Mk 57 VLS, pictured in Figure 12, employed by the Zumwalt-class destroyer is also intended to maximize the flexibility and adaptability of the shipboard weapon systems by employing electronics and software that use an open computing architecture.

Conceptually similar in construction to the Mk 41 VLS, the Mk 57 VLS is assembled with identical four-cell modules, which can use the current inventory of Mk 41 encanistered missiles and potentially even larger missiles. Unlike the Mk 41 VLS, the Mk 57 VLS was designed to be installed



BAE Systems

Figure 11: VLS Encanistered Missiles.

on the ship periphery instead of in centralized magazines. The Mk 57 VLS functional architecture is partitioned into four primary assemblies that manage and maintain the missile inventory and launch functions [6].

The Canister Electronic Unit (CEU) provides the “any-missile-in-any-cell” capability required by Navy VLSs. The CEU connects to an encanistered missile, interfacing the missile with the ship’s combat system. In essence, the missile

is simply a client on the weapons systems network. A Module Controller Unit (MCU) is provided to manage the launcher module and launcher equipment, monitor missile and canister activity, and detect and report faults and hazards. The transfer and monitoring of ship power to both the launcher and the missiles is provided by the Power Distribution Unit (PDU). And a Hatch Control Assembly (HCA) provides the motion and motor drive control required to actuate the launcher’s missile and exhaust hatches.

The Mk 57 VLS employs a gas management system that is a departure from the gas management system of the Mk 41 VLS. The Mk 57 reportedly uses a U-shaped gas management system that facilitates the egress of rocket motor exhaust gas through the uptake while mitigating the flow of hot gas into adjacent cells and the reversed flow into the active cell. This new gas management design is reported to be capable of accommodating new missile designs having up to a 45% greater rocket motor mass flow rate than rocket motors currently in use in U.S. VLSs. A reported advantage of this design is the elimination of a missile deluge system such as the system used in the Mk 41 VLS [8]. Elimination of the deluge system not only reduces maintenance requirements; it also eliminates the risk of an inadvertent deluge of a missile.

FUTURE TRENDS

Industry attempts to leverage R&D investments in both the Mk 41 and Mk 57 VLSs are ongoing. For



Figure 12: Mk 57 VLS.

example, an endeavor pursued by Lockheed Martin includes integrating nontraditional missile classes into the Mk 41 and Mk 57 launchers. The ExLS, pictured in Figure 13, fits within the volume of a standard VLS cell and incorporates a munitions adapter that mechanically retains multiple smaller munitions in a qualified All-Up-Round (AUR) configuration. The ExLS reportedly supports its own launch sequencing electronics and power supplies and has the ability to interface directly with the launch control computers of either the Mk 41 or Mk 57 VLSs [7]. The system appears to be marketed as a capability that can be dropped into existing launchers, but it is not clear how new physically integrated

The Mk 41 VLS was purposefully designed to support a common modular architecture with a high degree of commonality and interchangeability.

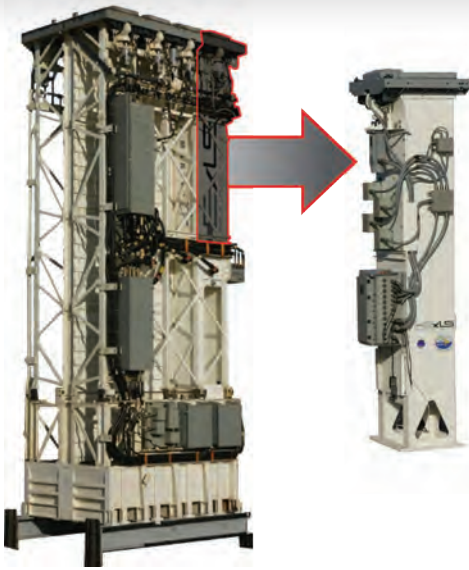


Figure 13: Lockheed Martin ExLS.

weapons will work with the legacy weapon control systems of CGs and Arleigh Burke/Zumwalt DDGs without the need for significant modifications

to the existing weapon control system or a new system altogether.

In any case, defense contractors Lockheed Martin and MBDA remain bullish and are pursuing efforts to integrate European missiles in the US Mk 41 VLS. The team recently demonstrated the ability to integrate and launch a European naval variant of the Common Anti-Air Modular Missile (CAMM), or Sea Ceptor, in a Mk 41 equipped with the ExLS. In this demonstration, the Sea Ceptor was cold-launched, as pictured in Figure 15, from its own canister with a gas ejection system and launch sequence that bypassed the commonly used Mk 41 LSEQ. Such a development is welcome news to the growing number of international navies employing the Mk 41 VLS, as this capability may provide the

needed flexibility to use missiles from different countries.

Another Lockheed Martin effort to leverage previously developed Mk 41 VLS technology was the development of a Single Cell Launcher (SCL). The SCL, pictured in Figure 14, maintains the form factor of the Mk 25 Quad Pack ESSM canister with a modified scalable mechanical structure. This design provides additional flexibility



Figure 14: Lockheed Martin SCL.

COLD LAUNCH VS. HOT LAUNCH

The VLS “cold launch vs. hot launch” debate has been gaining new momentum in recent years. Both system designs have their advantages and disadvantages. Hot launch systems have much faster engagement times as the missile is released from the ship almost immediately after the motor is ignited, whereas with a cold launch system, the missile must first be ejected from the launch cell and then ignited, thus extending the launch time. Further, cold launch systems do not require a hot exhaust gas management system but do require a gas, piston, or elevator ejection system, which could

introduce additional mechanical reliability concerns. The primary hazard with hot launch systems is the risk of a restrained firing (i.e., the missile rocket motor is ignited, but the restraint bolt[s] do not release). Likewise, cold launch systems have the risk of ejecting the missile without subsequent rocket motor ignition, potentially resulting in the ejected missile falling back onto the deck of the ship.

In either case, new hot/cold hybrid VLSs have gained renewed interest in both the United States and Europe. The feasibility of such a system was recently demonstrated by Lockheed Martin and MBDA when a Common Anti-Air Modular Missile (CAMM), or Sea Ceptor,

was cold-launched from the Mk 41 VLS (pictured in Figure 15) using the Lockheed Martin Extensible Launching System (ExLS).



Figure 15: Cold Launch.

for smaller platforms, such as frigates, patrol ships, and corvettes, where the size and weight of a traditional launcher module are of concern [8]. In fact, as pictured in Figure 16, Lockheed Martin has recently developed a concept for installing four SCLs in the Freedom Class Littoral Combat Ship (LCS) to enhance its combat capabilities.

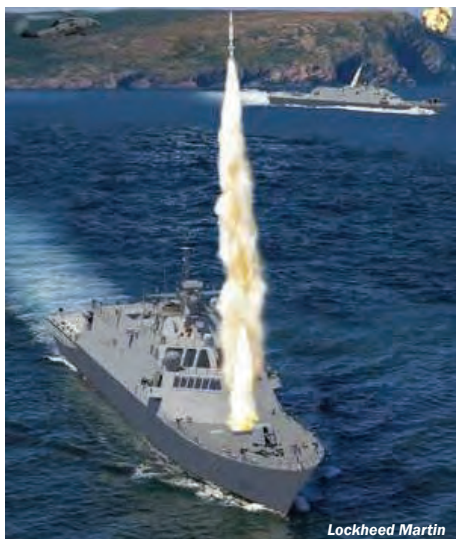


Figure 16: Freedom Class LCS with SCL Concept.

Nearly 90% of the SCL's components are common with the Mk 41 VLS, which should reduce the technical and logistical support burden and thereby minimize the overall life-cycle cost. And the SCL has been fully qualified for both performance and safety, including completing a demonstration of the system's ability to mitigate the hazards of a restrained firing.

In a more recent development, the Missile Defense Agency and the U.S. Navy successfully demonstrated the Department of Defense's (DoD's) ability to reuse and repurpose an

existing tactical system to perform a new mission. In May 2014, a BMD test was performed using a land-based variant of the Navy's Aegis Weapon System currently deployed on board certain ships. As mentioned previously, the system, called "Aegis Ashore," successfully fired a Standard Missile-3 Block IB guided missile from an Mk 41 VLS. The interoperability of Aegis systems should enable sea- and land-based systems, as illustrated in Figure 17, to work in concert to extend BMD coverage. Given the long, successful history of the Aegis system—and the fact that the system is currently in production and supporting both U.S. and international navies—the implications of the Aegis Ashore system demonstrating the same effectiveness as the sea-based system without having to invest in a new land-based system could be game-changing.

CONCLUSION

While the successes of the Mk 41 VLS could never be overstated, efforts to improve system

performance while continuing to reduce life-cycle cost must be the focus for the foreseeable future. The incorporation of "open" computing architectures into such systems has been, and continues to be, a necessary first step. But it's only a piece of the VLS cost puzzle, and additional standardization and COTS utilization is essential for further cost reductions. Much of the attention has been focused on ensuring the latest variants of the weapon and launch control computing and communication environments leverage COTS technology and employ open computing standards. However, when it comes to launcher electronics and the respective communication interfaces, the incremental advances that have been made remain incomplete.

Updating and standardizing the communication interfaces between the launch sequencer electronics and the missiles might be a logical next step. While this may be a difficult near-term investment, it may be necessary to realize significant cost savings in the future. For

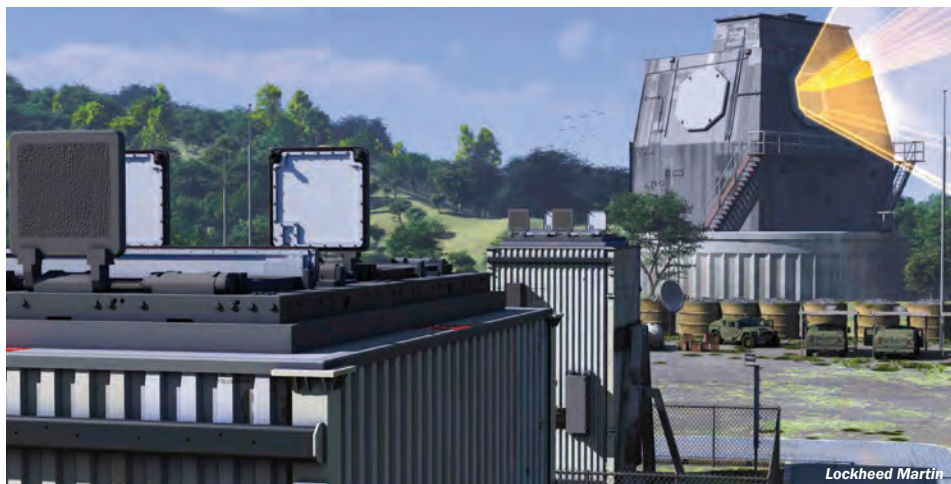


Figure 17: Aegis Ashore Concept.

example, the current umbilical cable to the missile canisters is a historical compilation of different custom communications protocols from RS- 232 to Mil-Std-1553, which generally only serve one missile class. Perhaps standardizing all U.S. Navy missile communication interfaces to a single protocol should be further analyzed. The latest Mk 41 VLS baseline design modularizes the launch sequence electronics to an individual cell. These electronics modules, which use the PC/104 embedded computer standard, are referred to as Cell Control Modules (CCM); and each is configured as a client in the missile launching network. The Baseline VII Mk 41 configuration has significantly improved COTS usage and missile availability, but each CCM still has a custom missile interface card for each missile class. And every umbilical to every missile canister remains bloated with a variety of missile communication interfaces regardless of the missile in the canister. Employing a standard missile communication interface would open the manufacturing of the electronic modules to more commercial competition while mitigating continuous issues with electronics obsolescence. Commercial industry could be positioned to more cost effectively manufacture generic electronic launch control modules and manage electronics obsolescence issues, allowing DoD contractors to focus on the more sensitive control software. With around 100 CCMs (including onboard repair parts) on a single DDG, the hardware savings could add up quickly. ■

BIOGRAPHY

ERIC FIORE, CSEP currently works for the SURVICE Engineering Company, where he is the Deputy Director of the Defense Systems Information Analysis Center (DSIAC). As a systems engineer for Lockheed Martin from 1999 to 2005, he was involved with the development of the Baseline VII Mk 41 VLS, including requirements development, system production, and ship integration activities. Mr. Fiore holds a B.S. in engineering science from Loyola University-Baltimore as well as an M.S. in electrical engineering from The Johns Hopkins University. He is an INCOSE Certified Systems Engineering Professional and a senior member of the Institute of Electrical and Electronic Engineers (IEEE).

REFERENCES

- [1] U.S. Department of the Navy. "US Navy Program Guide 2014." Washington, DC, 2014.
- [2] Lockheed Martin Corporation. "Mk 41 Vertical Launching System." Company brochure, Washington, DC, 2013.
- [3] Callinan, C. Personal Communication. Lockheed Martin Corporation, Fleet Support, 19 June, 2014.
- [4] Ciappi, J. Personal Communication. Lockheed Martin Corporation, Business Development, 8 August 2014.
- [5] Direction des Constructions Navales S.A. "Sylver." Company brochure, Paris, France, 2010.
- [6] Raytheon Corporation. "Mk 57 Vertical Launching System." Company brochure, Tewksbury, MA, 2007.
- [7] Lockheed Martin Corporation. "Extensible Launching System." Company brochure, Washington, DC, 2010.
- [8] Lockheed Martin Corporation. "Single Cell Launcher." Company brochure, Washington, DC, 2014.

ARTICLE SEARCH TERMS:

Navy Vertical Launching System VLS

RESULTS: 2,210

- Marine Engineering (255)
- Guided Missiles (246)
- Antimissile Defense Systems (191)
- Military Operations, Strategy, & Tactics (184)
- Theses (163)
- Weapon Systems (161)
- Logistics, Military Facilities, & Supplies (184)
- Defense Systems (137)
- Navy (136)
- Administration & Management (135)

***See page 3 for explanation ▶**

TRAINING

DSIAC provides a wide range of on-site and off-site training programs to Government and industry organizations. Our extensive technical knowledge, proven instructional expertise, and real-world experience in providing engineering and consulting services throughout DSIAC's technical scope areas results in training that is comprehensive, practical, and effective. The following are some of the training courses that DSIAC currently provides.

Accelerated Reliability Testing

<https://www.dsiac.org/training-courses/accelerated-reliability-testing> ▶

Achieving System Reliability Growth through Robust Design and Test

<https://www.dsiac.org/training-courses/achieving-system-reliability-growth-through-robust-design-and-test> ▶

Advanced Joint Effectiveness Model (AJEM) Training

<https://www.dsiac.org/training-courses/advanced-joint-effectiveness-model> ▶

Ground Vehicle Survivability and Force Protection Short Course

<https://www.dsiac.org/training-courses/ground-vehicle-survivability-and-force-protection-short-course> ▶

Mechanical Design Reliability

<https://www.dsiac.org/training-courses/mechanical-design-reliability> ▶

Reliability 101

<https://www.dsiac.org/training-courses/reliability-101> ▶

Software Reliability Testing and Security

<https://www.csiac.org/training-courses/software-reliability-testing-and-security> ▶

Weibull Analysis

<https://www.dsiac.org/training-courses/weibull-analysis> ▶

The next DSIAC open training will be in the winter of 2015.

CONFERENCES AND SYMPOSIA**NOVEMBER 2014****11th Avionics, Fiber-Optics & Photonics Conference**

11–13 November 2014

Hyatt Regency Atlanta
Atlanta, GAhttp://www.osa.org/en-us/meetings/global_calendar/events/11th_avionics_fiber-optics_photonics_conference/ ▶**Aircraft Survivability Technical Forum**

12–14 November 2014

Johns Hopkins University APL
Laurel, MD<http://www.ndia.org/meetings/5940/Pages/default.aspx> ▶**19th Annual Expeditionary Warfare Conference**

17–19 November 2014

Norfolk Marriott Waterside
Norfolk, VA<http://www.ndia.org/meetings/5700/Pages/default.aspx> ▶**12th Annual NanoTechnology for Defense Conference**

17–20 November 2014

Westfields Marriott Washington Dulles
Chantilly, VA<http://usasymposium.com/nano/> ▶**IEEE Green Energy and Systems Conference**

24 November 2014

Pyramid, California State University,
Long Beach
Long Beach, CAhttp://www.ieee.org/conferences_events/conferences/conferencedetails/index.html?Conf_ID=33476 ▶**MRS Fall Meeting & Exhibit**

30 November–5 December 2014

Hynes Convention Center & Sheraton
Boston Hotel
Boston, MA<http://www.mrs.org/fall2014/> ▶**DECEMBER 2014****I/ITSEC (Interservice/Industry Training, Simulation & Education Conference)**

1–4 December 2014

Orange County Convention Center
Orlando, FL<http://www.iitsec.org/Pages/default.aspx> ▶**Defense Logistics Conference**

2–4 December 2014

Hilton Alexandria Mark Center
Alexandria, VA<http://defenselogistics.wbresearch.com/agenda> ▶**Joint Army-Navy-NASA-Air Force (JANNAF)****46th Combustion/34th Airbreathing Propulsion/34th Exhaust Plume and Signatures/28th Propulsion Systems Hazards Joint Subcommittee Meeting**

8–11 December 2014

Hyatt Regency Albuquerque
Albuquerque, NM<https://www.jannaf.org/mtgs/Dec2014/pages/index.html> ▶**29th International Maintenance Conference**

8–12 December 2014

Hilton Daytona Beach Ocean Walk
Daytona, FL<http://imc-2014.com/> ▶**Combat Systems Symposium**

9–10 December 2014

JHU APL Kossiakoff Conference and Education Center
Laurel, MD<https://www.navalengineers.org/events/individualeventwebsites/Pages/CombatSystems2014.aspx> ▶**IEEE International Electron Devices Meeting**

15–17 December 2014

Hilton San Francisco
San Francisco, CAhttp://www.ieee.org/conferences_events/conferences/conferencedetails/index.html?Conf_ID=11149 ▶**JANUARY 2015****AIAA SciTech**

5–9 January 2015

Gaylord Palms and Convention Center
Kissimmee, FL<http://www.aiaa-scitech.org/> ▶**IEEE Radio and Wireless Symposium**

25–28 January 2015

Omni Hotel
San Diego, CAhttp://www.ieee.org/conferences_events/conferences/conferencedetails/index.html?Conf_ID=33207 ▶**26th Annual SO/LIC Symposium & Exhibition**

26–28 January 2015

Washington Marriott Wardman Park
Washington, DC<http://www.ndia.org/meetings/5880/Pages/default.aspx> ▶**61st Annual Reliability & Maintainability Symposium (RAMS)**

26–29 January 2015

Palm Harbor, FL

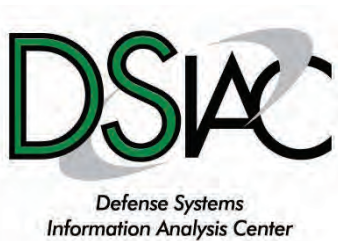
<http://rams.org/> ▶**39th Annual Conference on Composites, Materials, and Structures**

26–29 January 2015

Radisson Resort at the Port
Cocoa Beach, FL<http://advancedceramics.org/events/2014/01/27/conference/38th-annual-conference-on-composites-materials-and-structures/> ▶

Note: For the latest listing of events related to Defense Systems, please visit www.dsiac.org/events ▶





4695 Millennium Drive
Belcamp, MD 21017-1505



DSIAC ONLINE

www.dsiac.org

DSIAC PRODUCTS AND SERVICES INCLUDE:

- Performing literature searches.
- Providing requested documents.
- Answering technical questions.
- Providing referrals to subject-matter experts (SMEs).
- Collecting, electronically cataloging, preserving, and disseminating Defense Systems scientific and technical information (STI) to qualified users.
- Developing and deploying products, tools, and training based on the needs of the Defense Systems community.
- Fostering and supporting the DSIAC technical Communities of Practice.
- Participating in key DoD conferences and forums to engage and network with the S&T community.
- Performing customer-funded Core Analysis Tasks (CATs) under pre-competed IDIQ Delivery Orders.

DSIAC SCOPE AREAS INCLUDE:

- Advanced Materials
- Autonomous Systems
- Directed Energy
- Energetics
- Military Sensing
- Non-lethal Weapons
- Reliability, Maintainability, Quality, Supportability, and Interoperability (RMQSI)
- Survivability and Vulnerability
- Weapon Systems

